© 2015. Published by The Company of Biologists Ltd | Development (2015) 142, 702-711 doi:10.1242/dev.115832

RESEARCH ARTICLE

Plant embryogenesis requires AUX/LAX-mediated auxin influx

Hélène S. Robert[1,2,*], Wim Grunewald[1,*], Michael Sauer[3,4], Bernard Cannoot[1], Mercedes Soriano[5], Ranjan Swarup[6], Dolf Weijers[7], Malcolm Bennett[6], Kim Boutilier[5] and Jiří Friml[1,2,8,‡]

ABSTRACT

The plant hormone auxin and its directional transport are known to play a crucial role in defining the embryonic axis and subsequent development of the body plan. Although the role of PIN auxin efflux transporters has been clearly assigned during embryonic shoot and root specification, the role of the auxin influx carriers AUX1 and LIKE-AUX1 (LAX) proteins is not well established. Here, we used chemical and genetic tools on *Brassica napus* microspore-derived embryos and *Arabidopsis thaliana* zygotic embryos, and demonstrate that AUX1, LAX1 and LAX2 are required for both shoot and root pole formation, in concert with PIN efflux carriers. Furthermore, we uncovered a positive-feedback loop between MONOPTEROS (ARF5)-dependent auxin signalling and auxin transport. This MONOPTEROS-dependent transcriptional regulation of auxin influx (AUX1, LAX1 and LAX2) and auxin efflux (PIN1 and PIN4) carriers by MONOPTEROS helps to maintain proper auxin transport to the root tip. These results indicate that auxin-dependent cell specification during embryo development requires balanced auxin transport involving both influx and efflux mechanisms, and that this transport is maintained by a positive transcriptional feedback on auxin signalling.

KEY WORDS: *Arabidopsis thaliana* embryogenesis, Auxin transport, AUX1, LIKE-AUX1 (LAX), MONOPTEROS (ARF5), PIN, *Brassica napus*, Microspore

INTRODUCTION

Sexually reproductive organisms develop from a single-cell zygote, the product of fertilisation. Divisions of the zygote are precisely controlled in animals and plants and give rise to a population of cells that forms the embryo. In plants, embryos will develop a body plan along a shoot-root axis, containing one or two cotyledons, a shoot apical meristem, a hypocotyl and a root apical meristem. Notably, activation of transcriptional signalling pathways of the plant hormone auxin is pivotal for cellular patterning during embryogenesis (Rademacher et al., 2012; Schlereth et al., 2010; Weijers et al., 2006; Yoshida et al., 2014). However, auxins are not synthesized in all cells (Ljung et al., 2005; Petersson et al., 2009; Robert et al., 2013) and are therefore transported from source to sink tissues by specific influx and efflux proteins (Petrásek and Friml, 2009).

So far, it is assumed that the plasma membrane-localised PIN efflux proteins are responsible and rate-limiting for the directional auxin flow during embryogenesis (Friml et al., 2003; Weijers et al., 2006). Besides genetic and pharmacological evidence, this hypothesis is supported by the observation that auxin controls the direction of its own transport by regulating both the expression and localisation of PIN efflux transporters (Sauer et al., 2006a; Vieten et al., 2005). Recently, spatially and temporally defined foci of auxin production during embryogenesis were discovered to feed back on PIN proteins to regulate their polar localisation towards sink tissues, where auxin signalling triggers specific developmental programs (Robert et al., 2013; Wabnik et al., 2013). Also, indole-3-acetic acid (IAA), the major form of auxin, passively diffuses into the cytosol in its protonated form, suggesting that auxin efflux is the major mechanism for active auxin transport. However, in specific developmental situations, for example during root gravitropic responses (Swarup et al., 2001), lateral organ initiation and outgrowth (Kierzkowski et al., 2013; Swarup et al., 2008) and root hair development (Jones et al., 2008), passive auxin uptake needs to be supported by the amino acid permease-like proteins of the AUX1/LIKE-AUX1 (LAX) family (Bennett et al., 1996; Péret et al., 2012). A detailed analysis of these proteins during early embryogenesis has not been reported. So far, it was only demonstrated that members of the AUX1/LAX family are redundantly required for correct cell organisation in the radicle tip of mature embryos (Ugartechea-Chirino et al., 2009).

Here, we show that AUX1/LAX-dependent auxin influx is needed for cellular patterning from early embryogenesis onward and that the expression of *AUX1* and *LAX2* is controlled by the MP-BDL signalling pathway. We put forward a model in which auxin influx and efflux systems collaborate to regulate cell specification.

RESULTS

Microspore-derived embryos as a tool to study plant embryogenesis in high throughput

The study of molecular processes during plant embryogenesis is often limited by the relatively low sample numbers typically associated with laborious and technically challenging preparation methods. To overcome this limitation, we tested the potential of microspore-derived *in vitro* embryos of *Brassica napus* as an experimental system. Using heat-shock treatments together with specifically adjusted media, microspores isolated from early stage *B. napus* flowers can be induced to develop into suspensor-like structures, mimicking zygotic embryos (supplementary material Fig. S1) (Joosen et al., 2007; Supena et al., 2008). To test whether the microspore-derived *Brassica* embryos would respond in a similar way to zygotic *Arabidopsis* embryos, the effect of a collection of known chemicals on embryo development was investigated. The list consisted of the synthetic auxin analogues

[1]Department of Plant Systems Biology, Flanders Institute for Biotechnology (VIB) and Department of Plant Biotechnology and Bioinformatics, Ghent University, 9052 Gent, Belgium. [2]Mendel Centre for Genomics and Proteomics of Plants Systems, CEITEC MU – Central European Institute of Technology, Masaryk University, 625 00 Brno, Czech Republic. [3]University of Potsdam, Institute of Biochemistry and Biology, D-14476 Potsdam, Germany. [4]Departamento Molecular de Plantas, Centro Nacional de Biotecnología, Consejo Superior de Investigaciones Cientificas, 28049 Madrid, Spain. [5]Wageningen University and Research Centre, P.O. Box 619, 6700 AP Wageningen, The Netherlands. [6]School of Biosciences and Centre for Plant Integrative Biology, University of Nottingham, Nottingham LE12 5RD, UK. [7]Laboratory of Biochemistry, Wageningen University, 6703 HA Wageningen, The Netherlands. [8]Institute of Science and Technology Austria (IST Austria), 3400 Klosterneuburg, Austria.
*These authors contributed equally to this work

[‡]Author for correspondence (jiri.friml@ist.ac.at)

Received 28 July 2014; Accepted 21 December 2014

Development (2015) 142, 702-711 doi:10.1242/dev.115832

NAA and 2,4-D, the auxin antagonist PEO-IAA (Hayashi et al., 2008), the cytokinin BA, auxin transport inhibitors NPA and NOA, and chemicals affecting intracellular protein trafficking [brefeldin A (BFA), tyrphostin A23 and wortmannin].

The majority of the microspores cultivated in the presence of 0.1 µM 2,4-D developed into embryos with cotyledon and root pole specification defects (68/82; supplementary material Fig. S2B). In the presence of 1 µM 2,4-D there was an increase in the number of ball-shaped embryos (26/62; supplementary material Fig. S2C). Incubation of developing embryos in 0.1 or 1 µM NAA did not lead to obvious developmental defects, except for a mild increase in the number of ball-shaped embryos (5/67 or 6/71, respectively, as compared with 3/154 for the DMSO control; supplementary material Fig. S2L). In line with the reported role of auxin during *Arabidopsis* zygotic embryogenesis (Friml et al., 2003), treatments with the auxin antagonist PEO-IAA completely blocked *Brassica* microspore embryogenesis, even at low concentrations (supplementary material Fig. S2K). The same was observed by adding wortmannin, which is a strong inhibitor of intracellular protein trafficking, to the developing embryo cultures (data not shown). Also, tyrphostin A23, which is an inhibitor of endocytosis, strongly affected microspore embryogenesis (supplementary material Fig. S2L).

Blocking auxin transport by treating the *Brassica* microspore embryos with the auxin efflux inhibitor NPA induced severe patterning defects. At low concentrations (1 µM), NPA interfered with cotyledon initiation and development (31/62), whereas at higher concentrations (10 µM) it additionally affected apical-basal axis establishment, as demonstrated by the formation of ball-shaped embryos (12/55; supplementary material Fig. S2G,H). Very similar results were obtained with BFA (supplementary material Fig. S2D,F), a fungal toxin that affects intracellular trafficking of the PIN auxin transporters (Geldner et al., 2001). Interestingly, the phenotypes induced by 2,4-D, NPA and BFA resembled those observed in *Arabidopsis* auxin transport mutants or upon applying the same compounds to *Arabidopsis in vitro* ovule cultures (Friml et al., 2003). Also, for the cytokinin BA, which was previously shown to enhance the degradation of PIN transporters during *Arabidopsis* lateral root initiation (Marhavy et al., 2011, 2014) and to repress *PIN* expression in the *Arabidopsis* main root meristem (Růzicka et al., 2009), developmental defects were observed that can be related to a deficient auxin transport system. Incubation of developing microspores in 1 µM BA induced the formation of triangular embryos with a strong similarity to the 2,4-D-treated embryos (supplementary material Fig. S2I).

Thus, these observations show that *B. napus* microspore-derived embryos responded to the tested compounds in a very similar way to *Arabidopsis* zygotic embryos and suggest that the mechanisms that control auxin transport, which are intensively studied in *Arabidopsis*, are conserved in *B. napus*.

Pharmacological and genetic inhibition of auxin influx affects plant embryogenesis

Of all the compounds tested, the results obtained with the auxin influx inhibitor 1-naphthoxyacetic acid (1-NOA) (Parry et al., 2001) were not anticipated, as a role for auxin import during early embryogenesis has not been reported. After adding 1-NOA to microspore embryo cultures, an enhanced frequency of embryos with cotyledon specification and/or root specification defects was observed (60/153, as compared with 21/186 for the DMSO control; Fig. 1A-C; supplementary material Fig. S3). Since it is known that 1-NOA also partially reduces the activity of auxin efflux carriers (Lanková et al., 2010), we performed an NAA complementation

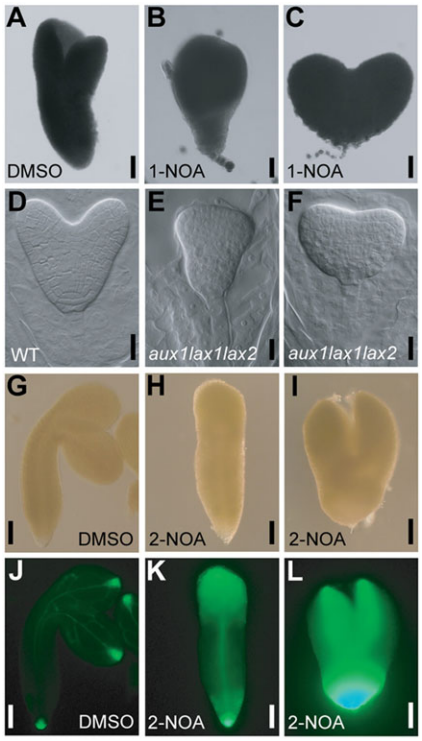

Fig. 1. Auxin influx is required for proper embryogenesis. (A-C) *Brassica napus* microspore embryos treated with 1-NOA (B,C) displayed fused cotyledons (B) and aberrant root development (C) phenotypes. (D-F) *Arabidopsis thaliana* zygotic embryos of wild type (WT; D) and *aux1 lax1 lax2* triple mutants (E,F) at heart stage. The mutant phenotypes resemble those of *B. napus* microspore embryos cultured in the presence of 1-NOA. (G-L) *A. thaliana* zygotic embryos cultured in the presence of 2-NOA (H,I,K,L) displayed fused cotyledons (H,K) and aberrant root development (I,L) phenotypes. Light (G-I) and fluorescence (J-L) images are shown of the *pDR5rev::GFP* signal in the same embryos. DMSO-treated controls are shown in A,G,J. Scale bars: 50 µm in A-C; 20 µm in D-L.

treatment. Uptake of the synthetic auxin NAA is independent of auxin influx carriers (Delbarre et al., 1996) and should therefore rescue auxin influx inhibitor-related defects. Interestingly, the 1-NOA/NAA double treatment did not impact the root specification defects, but rather reduced the frequency of embryos of small size or with fused cotyledons (4/88 for NOA/NAA treatment as compared with 23/153 for NOA alone; supplementary material Fig. S3).

Alternatively, we used 2-NOA, which has been shown to inhibit auxin import more specifically (Lanková et al., 2010), and found that 2-NOA mainly affected cotyledon development (26/119; supplementary material Fig. S3). Similar experiments were performed in *Arabidopsis* ovules cultured on 2-NOA for 3 and 5 days. In contrast to *Brassica* microspore embryos, for which treatment started after microspore induction, *Arabidopsis* ovules were cultured starting from later embryonic stages, about 3-4 days after pollination, when the majority of the embryos were at the early globular stage. *Arabidopsis* ovules treated with 2-NOA produced embryos with weak cotyledon and root phenotypes (7/25=28% for 3-day and 25/60=41.7% for 5-day treatment, as compared with 1/33=3.0% and 5/47=10.6%, respectively, for the DMSO control; Fig. 1G-I). The defects resembled those of *Brassica* microspore embryos cultured in the presence of NOA, i.e. smaller or fused cotyledons or aberrations at the root pole. In these embryos, the expression of the *DR5* auxin response marker (Friml et al., 2003; Ulmasov et al., 1997) was enhanced and more diffuse compared

Development (2015) 142, 702-711 doi:10.1242/dev.115832

with DMSO-treated embryos (Fig. 1J-L), possibly because disturbance of auxin influx by application of 2-NOA in post-globular embryos, in which the auxin response maximum is already established in the future root pole (Friml et al., 2003; Wabnik et al., 2013), may lead to a more diffuse auxin distribution (Bainbridge et al., 2008).

Taken together, these experiments show that pharmacological inhibition of auxin influx in *Brassica* microspore embryos and zygotic *Arabidopsis* embryos affects cotyledon development. Moreover, the defects in root development after NOA treatment, which were not rescued by NAA co-treatment, seemed indirectly linked to auxin influx defects and appeared to be a consequence of perturbed auxin distribution that affected auxin signalling. These data identify a novel role for auxin import in embryo patterning during plant embryogenesis, probably by ensuring the proper distribution of embryonic auxin.

AUX1, LAX1 and LAX2 are redundantly required for *Arabidopsis* embryo development

To study the putative role of auxin import during embryogenesis in more detail, we first determined which of the four members of the *Arabidopsis AUX/LAX* family of auxin influx carriers are expressed during embryogenesis. Expression analysis using a translational fusion reporter line (*pAUX1::AUX1-YFP*; Swarup et al., 2004), immunolocalisation (*pAUX1::AUX1-HA*; Swarup et al., 2001) and *in situ* mRNA hybridisation revealed a specific *AUX1* expression pattern in the inner cells at the 32-cell embryo stage and later in the provascular cells (Fig. 2A,B; supplementary material Fig. S4A). A similar expression domain was observed for *LAX2*, using *LAX2* transcriptional (*pLAX2::GUS*; Bainbridge et al., 2008) and translational (*pLAX2::LAX2-Venus*; Péret et al., 2012) reporter lines and immunolocalisation with a specific anti-LAX2 antibody (Péret et al., 2012). *LAX2* was expressed in provascular cells from the 32-cell stage onwards (Fig. 2I,J; supplementary material Fig. S4C, G-I). Additionally, *LAX2* expression was also detected in the hypophysis and the uppermost suspensor cells (Fig. 2I,J; supplementary material Fig. S4H,I). The earliest suspensor-specific *LAX2* expression was detected at the 16-cell stage (Fig. 2G,H; supplementary material Fig. S4B). In contrast to *AUX1* and *LAX2*, *LAX1* was expressed from the 1-cell stage onwards (*pLAX1::GUS*, *pLAX1::LAX1-Venus*; Bainbridge et al., 2008; Péret et al., 2012). *LAX1* expression was specific to the apical cell and was restricted to the proembryo until the 16-cell stage (Fig. 2C,D; supplementary material Fig. S4D). From the 32-cell stage onwards, it gradually became more pronounced in the upper tier (Fig. 2E; supplementary material Fig. S4E), consistent with its expression in the upper half of heart stage embryos including the cotyledons (Fig. 2F; supplementary material Fig. S4F). No *LAX3* expression could be detected during any stage of embryogenesis (data not shown), consistent with available seed-specific microarray data (Belmonte et al., 2013; Le et al., 2010).

Next, embryo development in the *aux/lax Arabidopsis* mutants was investigated. No obvious developmental defects were observed in the *aux1*, *lax1*, *lax2* single mutants or in *aux1 lax2* and *lax1 lax2* double mutants. Patterning defects in the upper tier as well as in the future root pole could be detected in the *aux1 lax1* double mutant, but with low penetrance (6/150=4%; Fig. 3C,M, Table 1). Interestingly, both the frequency (77/349=22.1%) and severity of the defects (Fig. 3) increased significantly in *aux1 lax1 lax2* triple-mutant embryos, demonstrating a functional redundancy between members of the AUX/LAX family in mediating embryo development. *aux1 lax1 lax2* embryos up to the globular stage showed defects in apical-basal axis establishment (11/125=8.8%; Fig. 3D) as manifested by aberrant division of the uppermost suspensor cells, giving the embryos an elongated shape and an unclear boundary between proembryo and suspensor. The most obvious defect observed from the early heart stage was the vertical symmetric instead of horizontal asymmetric division of the hypophysis (21/192=10.9%; Fig. 3E). Older embryos were much more affected and resembled *Brassica* microspore embryos grown in the presence of NOA (Fig. 1). Severe defects affecting both cotyledon and root development were observed (Fig. 3G-K,M-P). Consistently, these phenotypes were also reflected at the seedling stage, with a penetrance between 15 and 30% (Fig. 3Q,R). In line with the absence of *LAX3* expression, no additional effect was observed in *aux1 lax1 lax2 lax3* quadruple mutants as compared with *aux1 lax1 lax2* triple-mutant embryos, or in *lax1 lax2 lax3* as compared with *lax1 lax2* mutants (Fig. 3, Table 1). Taken together, these observations show that the differentially expressed auxin influx carriers are involved in embryo development.

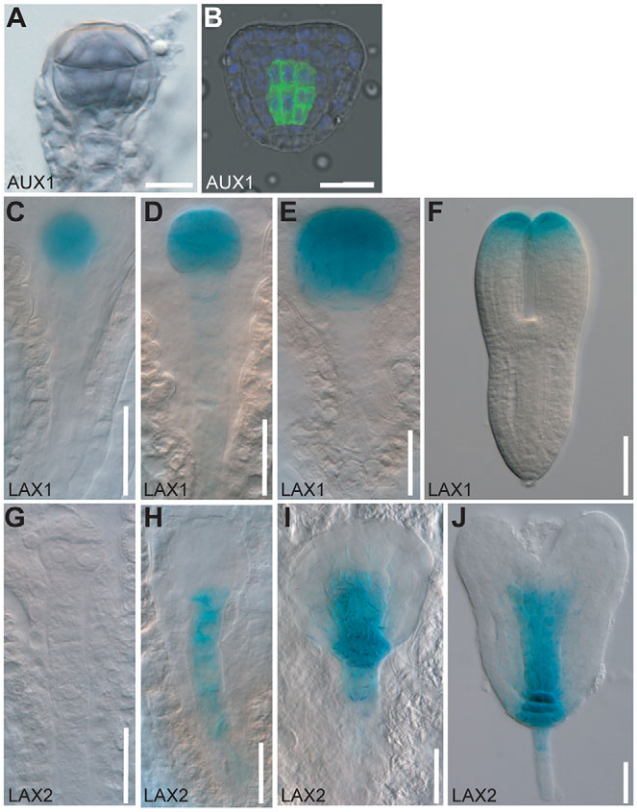

Fig. 2. *AUX1*, *LAX1* and *LAX2* are expressed during embryogenesis. *AUX1* (A,B), *LAX1* (C-F) and *LAX2* (G-J) are expressed during *Arabidopsis* embryo development. *AUX1* is expressed from the 32-cell stage in the inner cells, as detected by RNA *in situ* hybridisation (A, purple signal) and upon immunolocalisation of the YFP tag using anti-GFP antibodies in *pAUX1::AUX1-YFP* embryos (B, green signal; nuclei are stained in blue). *LAX1* is expressed in the proembryo from the 1-cell stage (C) until the early globular stage (D). Its expression is then progressively enhanced in the apical embryo tier at the late globular stage (E) and restricted to the cotyledon tips at the heart stage (F, late heart), as detected in *pLAX1::GUS* embryos. *LAX2* is first expressed in suspensor cells at the globular stage (H). No expression in detected before this stage, as illustrated in an 8-cell embryo (G). *LAX2* expression shifts to the provascular cells from late globular/transition stage (I), as detected in *pLAX2::GUS*. (J) Late heart stage. Scale bars: 20 µm.

Development (2015) 142, 702-711 doi:10.1242/dev.115832

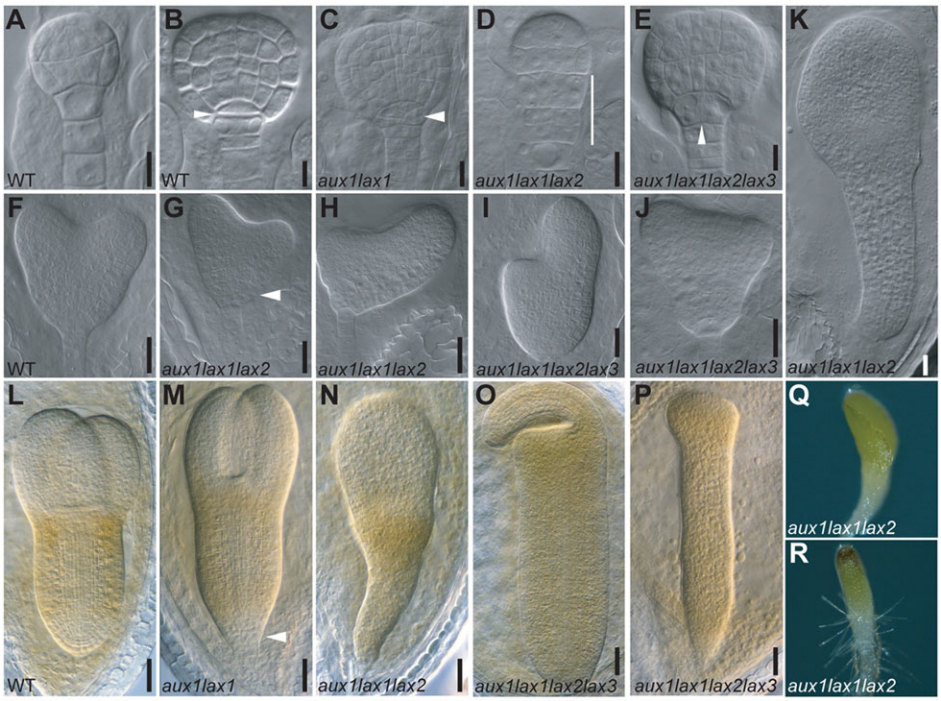

Fig. 3. *aux1*, *lax1* and *lax2* mutations affect both cotyledon and root formation. (A-P) *Arabidopsis* embryo development (A,D, early globular; B,C,E, late globular; F-J, heart; K-P, torpedo stages) is defective in different combinations of *aux*/*lax* mutations. These phenotypes are observed in each genotype at various penetrances. WT embryos are shown for comparison (A,B,F,L) with *aux1 lax1* (C,M), *aux1 lax1 lax2* (D,G,H,K,N) and *aux1 lax1 lax2 lax3* (E,I,J,O,P). (Q,R) Examples of *aux1 lax1 lax2* seedling phenotypes: a stubby hypocotyl (R) and monocotyledon with an underdeveloped root (Q). Arrowheads (C,E,G,M) and white line (D) indicate deviation from WT development. Scale bars: 10 µm in A-E; 20 µm in F-J; 50 µm in K-P.

Auxin influx and efflux as equivalent partners in the auxin flow towards the future root pole

Based on the expression patterns of *AUX1*, *LAX1* and *LAX2* at the globular stage, we speculated that these proteins would contribute to the auxin flow from the future shoot meristem towards the hypophysis or future root pole. To investigate this, expression of the auxin response reporter *pDR5rev::GFP* (Friml et al., 2003) was examined in the *aux1 lax1 lax2 lax3* background. Whereas wild-type embryos accumulate a strong GFP signal at the hypophysis (Fig. 4A), 29.2% (*n*=113) of *aux1 lax1 lax2 lax3* embryos showed a reduced *DR5* reporter activity (Fig. 4B). These results suggest that AUX/LAX-mediated auxin transport contributes to the auxin flow towards the future root pole.

Table 1. Summary of embryo phenotypes of *aux*/*lax* mutant combinations

Line	Phenotype	*n*	Embryo defects from late globular stage on (%)	References for the line
aux1	None	465	0	Bennett et al., 1996
lax1	None	233	0	Bainbridge et al., 2008
lax2	None	165	0	Bainbridge et al., 2008
aux1 lax1	Low penetrance for shoot and root specification defect	150	4	This study
aux1 lax2	None	360	0	This study
lax1 lax2	None	187	0	This study
lax1 lax2 lax3	None	205	0	This study
aux1 lax1 lax2	Enhanced penetrance and strength of *aux1 lax1* phenotypes	349	22.1	Bainbridge et al., 2008
aux1 lax1 lax2 lax3	No additive effects to *aux1 lax1 lax2*	208	23.1	Bainbridge et al., 2008

Similar problems in building a strong and focussed auxin signalling maximum in the hypophysis have been seen in *pin4* embryos (Friml et al., 2002) and in embryos with a reversed PIN1 polarity (Friml et al., 2004). Therefore, we tested the genetic interaction between the *AUX/LAX* and *PIN1/PIN4* genes. The embryonic phenotype was assayed at two locations: at PSB, Ghent, Belgium, and at CEITEC/MU, Brno, Czech Republic. We noticed that the phenotype penetrance was lower in Brno, where the multiple mutants were analysed. Possible reasons for these differences and incomplete penetrance are many, ranging from the quality of soil, water and light to the stability of growth temperature, pest control and watering frequency – especially in view of the susceptibility of auxin production to stress and growth conditions. In supplementary material Table S1, the phenotype percentages are detailed according to the growth location; those presented in the text below were obtained from plants grown in Brno.

In the progeny of *pin1-201*/+ plants, 12.5% (*n*=353) of the embryos showed defects during cotyledon development, whereas root pole defects were only occasionally observed (supplementary material Table S1). In the *aux1 lax1 lax2* background, 8.1% (*n*=459) of the embryos were affected in cotyledon (1.1%) and/or root pole (7%) formation (supplementary material Table S1). The total frequency of embryo defects in *pin1*/+ single, *aux/lax* triple and *pin1*/+ *aux1 lax1 lax2* quadruple mutants was comparable [12.5% (*n*=353), 8.1% (*n*=459) and 14% (*n*=129), respectively; supplementary material Table S1]. Interestingly, the majority of the defective *pin1 aux1 lax1 lax2* embryos had a *pin1*-like phenotype (12.4%), i.e. defects in cotyledon formation rather than root pole

Development (2015) 142, 702-711 doi:10.1242/dev.115832

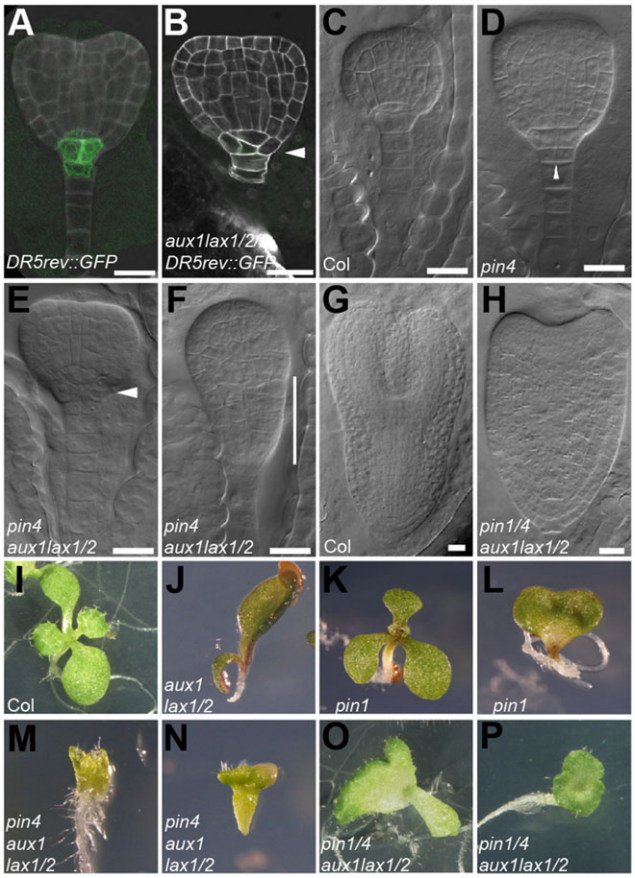

Fig. 4. *pin1* and *pin4* mutations rescue *aux/lax* root phenotypes. (A,B) *pDR5rev::GFP* auxin reporter expression is reduced in *aux1 lax1 lax2 lax3* embryos (B) as compared with WT *Arabidopsis* (A). (C-H) Embryo phenotype observed in *pin4* (D; arrowhead points to cell division in the uppermost suspensor cell), *pin4 aux1 lax1 lax2* (E,F) and *pin1/+ pin4 aux1 lax1 lax2* (H). WT embryos are shown for comparison (C,G). (I-P) After germination, seedlings of *aux1 lax1 lax2* (J), *pin1-201* (K,L), *pin4 aux1 lax1 lax2* (M,N), *pin1/+ pin4 aux1 lax1 lax2* (O), *pin1 pin4 aux1 lax1 lax2* (P) are affected in cotyledon and root development. A WT seedling is shown for comparison (I). Arrowheads (B,D,E) and white line (F) indicate deviation from WT development. Scale bars: 20 µm.

defects. This suggests that the *pin1* mutation rescues the root pole defects in *aux1 lax1 lax2* mutant embryos. Similar observations were made using *pin4*. In *pin4-2* single mutant embryos only subtle patterning defects in root and shoot were observed (2.1%, *n*=140), including premature divisions of the hypophysis daughter cells and vertical divisions of the uppermost suspensor cells (Fig. 4D). However, adding the *pin4-2* mutation to the *aux1 lax1 lax2* triple mutant rescued the developmental defects from 8.1% (*n*=459) to 4.9% (*n*=304) (Fig. 4E,F; supplementary material Table S1). Since PIN4 has been shown to partially compensate for the loss of PIN1 (Vieten et al., 2005), we also generated the quintuple mutant *pin1-201/+ pin4-2 aux1 lax1 lax2* and analysed its embryo development. Of embryos from *pin1/+ pin4 aux1 lax1 lax2* plants, 25.8% displayed defects in cotyledons but only 0.6% in roots (*n*=1424, 18 plants; Fig. 4H; supplementary material Table S1). In the quadruple *pin4 aux1 lax1 lax2* plants, among progeny of the same quintuple mother plant segregating for the *pin1-201* mutation, only 4.1% and 1% (*n*=432) of the embryos displayed cotyledon and root defects, respectively. Furthermore, *pin1/+ pin4 aux1 lax1 lax2* seedlings did not have cotyledons and the first true leaves were fused (12.6%, *n*=1978, seeds from 15 plants; Fig. 4P). Genotype analysis of 34 of these seedlings indicated that this phenotype was present in homozygous *pin1 pin4 aux1 lax1 lax2* quintuple mutants. In addition, aberrant cotyledon development was observed in 5.9% of the *pin1/+ pin4 aux1 lax1 lax2* seedlings (Fig. 4O compared with *pin1* in Fig. 4K,L), which is a similar proportion to that in the *pin4 aux1 lax1 lax2* population (from plants segregating for the *pin1-201* mutation) (4.4%, *n*=424, seeds from four plants; Fig. 4M,N; supplementary material Table S2). Notably, the root phenotype observed in *aux1 lax1 lax2* seedlings (4.8%, *n*=289; Fig. 4J) was gradually rescued when the *pin* mutations were introduced: 0.6% (*n*=349) in *pin4 aux1 lax1 lax2*, 0.5% (*n*=554) in *pin1/+ aux1 lax1 lax2* and 0.1% (*n*=1978) in *pin1/+ pin4 aux1 lax1 lax2* (supplementary material Table S2).

Taken together, these genetic analyses show that the different *aux/lax* and *pin* mutations have additive effects on cotyledon formation and thus indicate that both auxin influx and efflux carriers play a role in this auxin transport-dependent developmental event. However, re-equilibrating auxin transport towards the root pole in *aux/lax* mutants by introducing mutations in efflux carriers rescued the root defects in these embryos, suggesting that proper auxin signalling for root pole specification might be restored in the quintuple mutant.

AUX/LAX-mediated auxin import is controlled by the MP-BDL signalling pathway

The defects in the *aux/lax* triple-mutant embryos strongly resembled those reported for the auxin response mutants *monopteros* (*mp*) and *bodenlos* (*bdl*) (Berleth and Jürgens, 1993; Hamann et al., 1999). MP (also known as ARF5) is an auxin-responsive transcription factor that regulates auxin-dependent gene expression, while BDL (also known as AUX/IAA12) is an auxin-degradable repressor of MP activity. Using qRT-PCR, expression of the auxin influx carriers was analysed in seedlings expressing an inducible auxin-insensitive *bdl* mutant protein (Schlereth et al., 2010). In *pRPS5A::bdl-GR* seedlings, the expression of *AUX1*, *LAX2* and *PIN1* was less strongly induced than in the control (*pRPS5A::BDL-GR*, expressing the wild-type *BDL* gene) after 1 h DEX/NAA co-treatment (supplementary material Fig. S5A), whereas the expression of *LAX1* was less affected by this treatment. In line with this, *AUX1* and *LAX2* expression levels were reduced in the *mp* mutant, while *LAX1* expression was reduced but to a lesser extent (supplementary material Fig. S5A). To confirm the embryonic transcriptional regulation of *AUX1*, *LAX1* and *LAX2* by MP, transcriptional (*LAX1*, *LAX2*) and translational (*AUX1*) reporters were introduced into the *mp* strong mutant allele background (mp^{B4149}). Whereas *LAX1* expression was unaffected (Fig. 5D), that of *AUX1* and *LAX2* was reduced or absent in *mp* embryos (Fig. 5E,F).

Next, the genetic interaction between *MP* and the *AUX/LAX* genes was tested by generating multiple mutants. All mutants were screened for the frequency of *mp*-like defects during embryogenesis, as well as for the percentage of rootless seedlings. In both cases we observed that adding *aux1*, *aux1 lax2* or the *aux1 lax1 lax2* mutations to the incompletely penetrant *mp* allele mp^{S319} both qualitatively and quantitatively enhanced the *mp* phenotype (Fig. 5I,J; supplementary material Table S3). Based on these results we conclude that AUX1 and LAX2 act downstream of the MP-BDL signalling pathway.

Similar transcriptional regulation of the PIN1 auxin efflux carrier by the MP-BDL pathway has been demonstrated previously (Weijers et al., 2006). Since we showed that both auxin influx and efflux systems work together during embryo development, we examined the

Development (2015) 142, 702-711 doi:10.1242/dev.115832

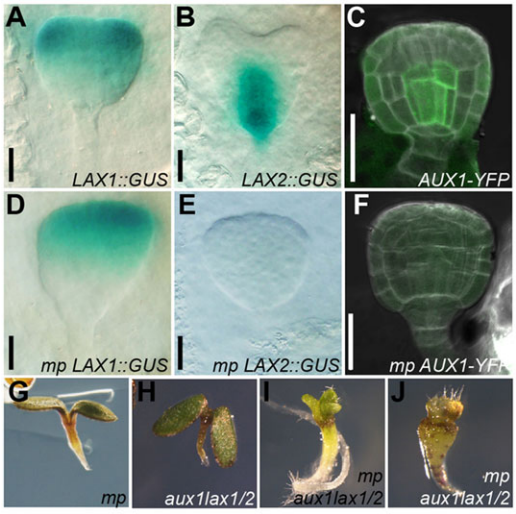

Fig. 5. MP-BDL transcriptional pathway regulates *AUX1* and *LAX2* expression. (A-F) *LAX2* (B,E) and *AUX1* (C,F), but not *LAX1* (A,D), expression is absent in mp^{B4149} embryos (D-F), as compared with WT *Arabidopsis* (A-C). (G-J) Seedling phenotypes of mp^{S319} (G), *aux1 lax1 lax2* (H) and mp^{S319}*aux1 lax1 lax2* (I,J). Scale bars: 20 µm.

extent to which they contribute to MP-mediated embryonic root formation. Both the strong (mp^{B4149}) and weak (mp^{S319}) *mp* alleles were transformed with *pMP::AUX1*, *pMP::LAX2* or *pMP::PIN1* constructs. The *mp*/+ T2 segregating lines were screened for the frequency of rootless seedlings (supplementary material Table S4). None of the constructs affected the percentage of rootless seedlings in the mp^{B4149} background: 25.7±3.7% in *mp*/+ *pMP::AUX1* (28 lines), 25.5±4.8% in *mp*/+ *pMP::LAX2* (31 lines) and 23.2±5% in *mp*/+ *pMP::PIN1* (13 lines), as compared with 24.9±2.6% in mp^{B4149}/+. However, in the mp^{S319} background, *MP* promoter-driven expression of the auxin transporters enhanced the frequency of rootless seedlings: 9.2±3.3% in *mp*/+ *pMP::AUX1* (33 lines), 13.7±6.5% in *mp*/+ *pMP::LAX2* (29 lines) and 9.6±4.3% in *mp*/+ *pMP::PIN1* (28 lines), as compared with 4.6±1.6% in mp^{S319}/+.

Given the cooperative role of auxin influx and efflux carriers, we anticipated that adding one auxin transport component is insufficient to complement the *mp* mutation and would moreover disturb the affected system even more. To test this hypothesis, *mp*/+ *pMP::AUX1* and *mp*/+ *pMP::LAX2* were crossed to *mp*/+ *pMP::PIN1* and F1 progenies were analysed (supplementary material Tables S5 and S6). F1 progeny of the crosses mp^{B4149}/+ *pMP::AUX1*×mp^{B4149}/+ *pMP::PIN1* and mp^{B4149}/+ *pMP::LAX2*×mp^{B4149}/+ *pMP::PIN1* produced a similar proportion of rootless seedlings as the control cross (supplementary material Table S5). When the same experiment was performed in the mp^{S319} background, the same trend was observed in F1 crossed seedlings and individual lines, i.e. an enhancement of the penetrance of mp^{S319} rootless phenotypes (supplementary material Table S6). We conclude that reconstituting either *AUX1* or *LAX2* and *PIN1* expression in the provascular expression domain of *mp* embryos is not sufficient to rescue the mp^{B4149} rootless phenotype, and even enhances mp^{S319} defects.

Altogether, these experiments showed that *PIN1*, *AUX1* and *LAX2* are under transcriptional control of the MP-BDL auxin-dependent signalling pathway, which is in line with earlier results for LAX2 (Schlereth et al., 2010). Genetic data suggest that the auxin transport machinery acts downstream of the MP-BDL signalling pathway for root pole formation. However, our attempts to rescue *mp* mutations by ectopic expression of auxin transport proteins indicated that restoring proper auxin transport machinery to the root pole is not sufficient to rescue impaired root development in these mutants.

DISCUSSION

While testing the utility of *B. napus* microspore embryos as a high-throughput assay system, we uncovered an unexpected role for auxin influx during early embryo development – unexpected, because auxin import during embryogenesis has been studied previously and only a role in mature embryos was reported (Ugartechea-Chirino et al., 2009). More precisely, it was demonstrated that *aux1 lax* mutants have a larger radicle root cap along with aberrant cellular organisation of the root tip. By investigating mature embryos only, the earlier role of AUX1/LAX family proteins has probably been overlooked. By performing transcriptional and genetic analyses in *A. thaliana* from fertilisation onwards, we demonstrated that all three auxin importers *AUX1*, *LAX1* and *LAX2* have specific expression patterns during early zygotic embryogenesis and that they act redundantly to specify embryonic root and shoot pole identity and development.

Brassica microspore embryos as a model to study *Arabidopsis* embryogenesis

Inhibiting auxin influx in *Brassica* embryos using 2-NOA affected cotyledon development. Because 1-NOA has been reported to affect efflux transport (Lanková et al., 2010) and since cellular uptake of NAA is independent of auxin influx carriers (Delbarre et al., 1996), a 1-NOA/NAA co-treatment was performed to dissect the actual effect of 1-NOA on auxin influx. This 1-NOA/NAA co-treatment confirmed the more specific action of 2-NOA and thus indicates that auxin influx in *Brassica* microspore embryos is mainly important for cotyledon development.

Switching from the *Brassica* system to *Arabidopsis* zygotic embryos, we were confronted with some phenotypic differences. Whereas *Brassica* microspore embryos treated with auxin import inhibitors were mainly affected in cotyledon development, *Arabidopsis aux/lax* mutant embryos were mainly affected in root pole formation and to a lesser extent in cotyledon development. However, given the similarity of the phenotypes and the rescue of the 1-NOA-dependent cotyledon phenotype by NAA treatment, these observations suggest that the defects in cotyledon development are specifically related to disturbed auxin influx machinery. Several reasons for the differences in *Brassica* and *Arabidopsis* phenotypes can be proposed: (1) the different genetic backgrounds; (2) the differences between pharmacological and genetic disturbance of auxin import action; (3) differences in developmental context regarding zygotic embryo development in the presence of sporophytic ovule tissue and endosperm versus the *in vitro* microspore context from which the *Brassica* embryos developed. Despite the phenotypic differences, the *B. napus* microspore embryo system provided an important initial indication for a role for auxin import in *Arabidopsis* embryo development. Moreover, the fact that we observed the expected phenotypic output of treatments with a palette of other compounds affecting various cellular processes shows that the *B. napus* system can be used for the pharmacological study of embryo development.

A cooperative role of auxin influx and efflux in embryogenesis

In 16-cell-stage *Arabidopsis* embryos the PIN1 auxin transporter switches from an apolar to a polar localisation (Friml et al., 2003; Robert et al., 2013; Wabnik et al., 2013). Correspondingly, a directed auxin flow from the future shoot meristem towards the root

Development (2015) 142, 702-711 doi:10.1242/dev.115832

pole is activated (Friml et al., 2003, 2004; Wabnik et al., 2013). Here, we showed that the expression of the auxin influx carrier *AUX1* is first detected in the central cells of a 32-cell stage embryo, together with *LAX2* expression from the 32-cell stage onwards. Given their spatial localisation pattern and their reported auxin import activity, we hypothesized that AUX1/LAX-mediated influx provides auxin to the provasculature for PIN1-mediated directional auxin flow towards the root pole (Fig. 6). Indeed, mutating *AUX1* and *LAX2* together with the functionally redundant *LAX1* importer revealed clear defects in root pole formation and to a lesser extent in cotyledon development. Also, the *DR5* auxin response marker was decreased in the root pole of *aux1 lax1 lax2 lax3* mutant embryos, suggesting a role for auxin influx in shoot pole-to-root pole auxin transport, as previously speculated (Spitzer et al., 2009). Interestingly, mutations in the *PIN1* auxin efflux carrier showed opposite developmental defects: mainly cotyledon defects and fewer defects at the root pole.

Combining mutations in both auxin efflux and influx carriers using quadruple and quintuple mutants would intuitively suggest stronger defects in both cotyledon and root pole developmental programs. However, whereas the *pin1 aux1 lax1 lax2* quadruple mutant showed increased penetrance of the cotyledon phenotype, it unexpectedly showed fewer defects in root development compared with *aux1 lax1 lax2*. An explanation might be found in the tissue-specific expression of the auxin transporters. While *PIN1*, *PIN4*, *AUX1*, *LAX2* are expressed in provascular cells, both *LAX1* and *PIN1* are also expressed in protoderm cells. In the protoderm layer, auxin is channelled from the suspensor to the cotyledon tips. Hence, in addition to a disturbed transport in the inner cells, upward auxin transport in the protoderm might also be affected in *pin/aux/lax* quadruple and quintuple mutants. We hypothesize that perturbing auxin transport in the protoderm might result in increased auxin accumulation in the suspensor and decreased auxin delivery to the apical regions, which would explain both the root phenotype rescue in *pin1 aux1 lax1 lax2* embryos and the enhanced frequency of cotyledon defects.

A positive transcriptional feedback of auxin signalling on auxin transport for root development

The MP-BDL-mediated signalling pathway has repeatedly been shown to be crucial for hypophysis specification and hence root pole formation. *MP* expression in the *AUX1/LAX2/PIN1* expression domain drives the expression of both influx and efflux carriers, AUX1, LAX2 and PIN1, which are needed to establish the essential auxin response maximum in the root stem cell niche (Fig. 6). The close relationship between auxin transport and auxin signalling is illustrated by the similarities in the *mp* and *aux1 lax1 lax2* mutant phenotypes. Therefore, we investigated the effect of restoring the expression of one or more auxin transport components in the *mp* mutant background. However, none of the combinations led to a reduced frequency of *mp*-like defects or to a reduction in mutant phenotypes. The most plausible explanation is that reactivation of auxin transport is not able to activate the expression of the MP target genes *TARGET OF MONOPTEROS 5* (*TMO5*) and *TMO7*, which have been shown to be involved in MP-controlled root pole development (Schlereth et al., 2010).

Interestingly, although reactivation of one of the auxin components in the *mp* background would intuitively lead to either a small rescue of the *mp* phenotype or to no change in phenotype, the transformed mp^{S319} mutants in fact showed an enhanced frequency of the *mp* phenotype, suggesting that the constructs enhanced the *mp*-related defects. We hypothesize that fully operational and balanced auxin transport in the embryo requires both PIN and AUX/LAX components. This conclusion is consistent with recent findings in *Arabidopsis* root apical tissues (Band et al., 2014). In *mp* embryos, PIN1-dependent efflux and AUX1/LAX2-dependent influx machineries are not functional (Fig. 5) (Weijers et al., 2006). Adding only one component, i.e. PIN or AUX/LAX, would then disturb the defective system even more. This can be compared to a traffic jam: if an obstruction blocks the road, opening the entrances upstream of the obstruction would only make the traffic jam worse.

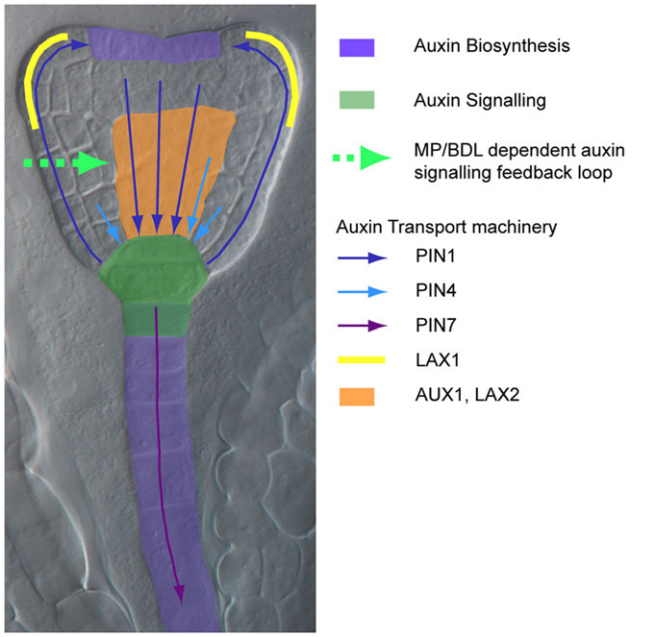

Fig. 6. Model for balanced and regulated auxin transport during embryo development. Local auxin production occurs in the two opposite poles of the embryo: in the suspensor and the shoot apical meristem. Auxin is transported by PIN1 and LAX1 from the suspensor to the tips of the cotyledons via the protoderm. Auxin is transported by efflux (PIN1 and PIN4) and influx (AUX1 and LAX2) transporters from the shoot apical meristem to the root meristem, where it accumulates and triggers auxin signalling. From the root meristem, auxin is transported away from the embryo by PIN7. Transcriptional feedback involving MP (dashed arrow) regulates expression of *PIN1*, *AUX1* and *LAX2* in the inner embryonic cells.

Concluding remarks

In this study, we showed the importance of auxin influx machinery for embryo development. In our attempts to uncouple the roles of the AUX/LAX proteins in cotyledon and in root development, we also identified a transcriptional feedback loop in which the MP-BDL auxin signalling pathway regulates *AUX1* and *LAX2* expression in the inner embryonic cells. Interfering with auxin transport from its source in the shoot apical meristem to the future root meristem resulted in aberrant root development. We also identified a cooperative role of auxin influx (LAX1) and efflux (PIN1) in cotyledon specification. Together, these results support the requirement of coordinated auxin influx and efflux for proper embryo development.

MATERIALS AND METHODS

Plant material and growth conditions

A. thaliana seeds were sterilised with chlorine gas, plated on half-strength Murashige and Skoog (MS) medium (pH 5.7) containing 1% sucrose, 0.01% myo-inositol, 0.05% MES and 0.8% agar, stored for 2 days at 4°C,

Development (2015) 142, 702-711 doi:10.1242/dev.115832

and grown vertically at 21°C under continuous light. Two weeks after germination, seedlings were transferred to soil and grown at 21°C under long-day conditions.

The following lines were described previously: *aux1-21*, *lax1*, *lax2*, *aux1 lax1 lax2*, *aux1 lax1 lax2 lax3*, *pin1-201*, *pin4-2*, *pin4-3*, mp^{B4149}, mp^{S319}, *pDR5rev::GFP*, *pLAX1::LAX1-VENUS*, *pLAX2::LAX2-VENUS*, *pLAX1::GUS*, *pLAX2::GUS*, *pLAX3::GUS*, *pAUX1::AUX1-HA*, *pAUX1::AUX1-YFP*, *pRPS5A::BDL-GR* and *pRPS5A::bdl-GR* (Bainbridge et al., 2008; Bennett et al., 1996; Cole et al., 2009; Friml et al., 2003; Furutani et al., 2004; Marchant et al., 1999; Péret et al., 2012; Swarup et al., 2004; Weijers et al., 2006). The following lines were generated by crossing: *aux1 lax1*, *aux1 lax2*, *lax1 lax2*, *lax1 lax2 lax3*, *pDR5rev::GFP aux1 lax1 lax2 lax3* [generated by crossing *DR5rev::GFP aux1 lax1 lax2* and *aux1 lax1 lax2 lax3* (Bainbridge et al., 2008)], *pin1-201 aux1 lax1 lax2*, *pin4-2 aux1 lax1 lax2*, *pin4-3 aux1 lax1 lax2*, *pin1-201 pin4-2 aux1 lax1 lax2*, mp^{S319} *aux1 lax1 lax2*.

Generation and analysis of ectopic expression of *PIN1*, *AUX1* and *LAX2* in the *mp* background

The *MP* promoter from the *pJet_MP*-promoter (kindly provided by the Dolf Weijers lab) vector was cloned into *pDONRP4P1R* (Karimi et al., 2007a) using primers attB4_MP_FOR and attB1R_MP_REV (see supplementary material Table S7). *PIN1*, *AUX1* and *LAX2* genomic DNA was amplified from *Arabidopsis* seedlings using primers (see supplementary material Table S7), and Gateway cloned in *pDONR221* (Karimi et al., 2007b). Using a multisite Gateway reaction, *PIN1*, *AUX1* and *LAX2* entry clones were combined with the *MP* promoter into *pH7m24GW* (Karimi et al., 2007a). Heterozygous mp^{B4149} and mp^{S319} plants were transformed by the floral dip method. T1 transformants were selected for the presence of mp^{B4149} and mp^{S319} mutations. Hemizygous T2 lines were analysed for *mp*-like phenotype penetrance. A selection of lines was tested for overexpression of the transgenes by qRT-PCR (see below), and grown to obtain T3 homozygous hemizygous *pMP:xx* in mp^{B4149}/+ and mp^{S319}/+ backgrounds. Phenotype penetrance was confirmed in T3 homozygous lines. T3 lines were used for crossing *PIN1* to *AUX1* or *LAX2* to simultaneously ectopically express efflux and influx auxin carriers in embryos. F1 seedling phenotypes were scored.

Microspore-induced embryogenesis and chemical treatments

The generation of embryos using double-haploid *B. napus* cv Topas DH4079 microspores was performed according to Supena et al. (2008). After collecting the microspores, a heat shock of 22 h at 32°C in the dark was applied using a microspore density of 40,000 per ml. Microspores were distributed in 24-well plates (500 µl per well) and incubated at 25°C in the dark. Five days after the heat shock, when the microspores had a swollen appearance, compounds (or mock) were added in 500 µl medium, bringing the total volume to 1 ml per well. This stage was selected to overcome a putative negative effect of the compounds on the microspore embryo induction program. Microspore embryogenesis was evaluated daily using light microscopy and phenotypes were quantified 7 days after treatment. Embryos ranged from globular to torpedo stages. The compounds used were: NAA (α-naphthaleneacetic acid; Duchefa), 2,4-D (2,4-dichlorophenoxyacetic acid; Sigma), PEO-IAA [α-(phenylethyl-2-one)-indole-3-acetic acid; a gift from Ken-Ichiro Hayashi, Okayama University of Science, Japan], BA (6-benzylaminopurine; Sigma), NPA (N-1-naphthylphthalamidic acid; Sigma), 1-NOA (1-naphthoxyacetic acid; Sigma), 2-NOA (2-naphthoxyacetic acid; Sigma), brefeldin A (Sigma), wortmannin (Sigma), tyrphostin A23 (Sigma) and tyrphostin A51 (Sigma). Stock solutions were diluted in DMSO.

In vitro culture of *Arabidopsis* embryos

Culture of embryos was carried out as previously described (Sauer and Friml, 2008). Culture medium was supplemented with 10 µM 2-NOA in DMSO, or the equivalent amount of DMSO as a solvent control. Seeds originating from siliques 3 and 4, counting from the first dehiscent flower, were cultured for 6 days. Embryos were extracted from the seeds for microscopy analysis. Only embryos from healthy seeds were analysed.

Histological analyses, *in situ* hybridisation and microscopy

For GUS staining, embryos were dissected out of the seeds in 90% acetone. For embryos younger than the globular stage, seeds were opened but the embryos were not dissected. After dissection, seeds and embryos were transferred to sieves (BD Falcon, cell strainer 40 µm nylon) and were incubated under vacuum for 10 min in 90% acetone. Subsequently, three washing steps were performed under vacuum for 10 min each with 0.5 M phosphate buffer [Na_2HPO_4/NaH_2PO_4 (615/385), pH 7]. Sieves were then transferred to GUS staining solution [1 mM X-Glu dissolved in 0.5% (v/v) DMFO, 0.5% (v/v) Triton X-100, 1 mM EDTA, 0.5 mM $K_3Fe(CN)_6$, 0.5 mM $K_4Fe(CN)_6$, 0.5 M phosphate buffer pH 7] and incubated for 1 h under vacuum. After vacuum infiltration, samples were incubated at 37°C. The staining reaction was stopped by two washes with 0.5 M phosphate buffer under vacuum for 10 min each. Embryos were transferred to slides, mounted with 10% glycerol and analysed with a DIC fluorescence microscope (Olympus).

Immunofluorescence analyses of *Arabidopsis* embryos were performed as previously described (Sauer et al., 2006b) using mouse anti-HA (1/600; 5B1D10, catalog number 32-6700, Life Technologies), rabbit anti-LAX2 (1/200; Péret et al., 2012), mouse anti-GFP (1/600; clone GFP-20, G6539, Sigma), Cy3-conjugated goat anti-mouse (1/600; polyclonal, C2181, Sigma) and anti-rabbit (1/600; polyclonal, C2306, Sigma), and Alexa488-conjugated goat anti-mouse (1/600; A-11001, Life Technologies). Nuclei were stained with DAPI (1 mg/l in water; Sigma).

For GFP visualisation, embryos were fixed in 4% PFA in PBS buffer (pH 7.4) and prepared on slides as described (Sauer et al., 2006b). Embryos were rehydrated in water, and when indicated stained for 2 h in SCRI Renaissance 2200 (Renaissance Chemicals; 2% in 4% DMSO/water solution), washed twice in water and mounted with an anti-fading solution.

For *Arabidopsis in vitro*-cultured embryos, GFP was visualised after dissection from the seed in a 5% glycerol/water solution.

For embryo phenotyping, embryos were cleared at the indicated stages in a chloral hydrate solution [chloral hydrate/water/glycerol (8/3/1, w/v/v)].

Whole-mount *in situ* hybridisation of embryos was carried out as previously described (Hejátko et al., 2006) using a full-length *AUX1* RNA probe (see supplementary material Table S7 for primer sequences). Embryos were analysed by clearing seeds in chloral hydrate.

Confocal imaging was performed on Zeiss Exciter 5, 710 and 780 confocal laser scanning microscopes using 405 nm (DAPI, Renaissance), 488 nm (YFP, GFP, Alexa488) and/or 543 nm (Cy3) excitation filters with 420-480 nm band pass (DAPI, Renaissance), 505-530 nm band pass (GFP, YFP, Alexa488) and 560 nm long-pass (Cy3) emission filters. Acquisition with multiple channels was performed by sequential scanning. Microscopy observations were performed on a DIC fluorescence microscope (Olympus). Images were processed in Adobe Photoshop CS and assembled in Adobe Illustrator CS.

RNA extraction, cDNA synthesis and qRT-PCR analysis

The experiment was set up according to Schlereth et al. (2010). *pRPS5A::BDL-GR*, *pRPS5A::bdl-GR*, mp^{B4149} and Col seedlings were grown for 5 days, treated in liquid medium with 10 µM dexamethasone (DEX; Santa Cruz) for 1 h, then co-treated with 10 µM NAA and 10 µM DEX for 1 h, 2 h or 4 h. Presented data are from 1 h co-treatment. For RNA extraction, whole seedlings were ground in liquid nitrogen and total RNA was isolated with Trizol (Invitrogen) according to the manufacturer's instructions. Poly(dT) cDNA was prepared from 2 µg total RNA with Superscript III reverse transcriptase (Invitrogen) and quantified on an LightCycler 480 apparatus (Roche Diagnostics) using the SYBR Green I Master Kit (Roche Diagnostics) according to the manufacturer's instructions. All individual reactions were carried out in triplicate. Primers are listed in supplementary material Table S7. Data were analysed with qBase (Hellemans et al., 2007). Expression levels of *AUX1*, *LAX1*, *LAX2*, *LAX3* and *PIN1* were normalised to those of *EEF1α4* and *CDKA*, which showed no clear systematic changes in Ct values. Data from *BDL-GR* were compared with *bdl-GR* and data from *mp* were compared with Col.

Statistical analysis

Statistical analysis was performed by contingency table χ^2 tests. Details are provided in supplementary material Tables S1-S6.

Acknowledgements
We thank Cris Kuhlemeier and Ken-Ichiro Hayashi for providing material; Agnieszka Bielach for support with statistical analysis; and N. Smet and the PSB transformation facility for technical assistance.

Competing interests
The authors declare no competing or financial interests.

Author contributions
W.G., H.S.R. and J.F. designed the project. W.G. performed the *Brassica* microspore embryo related work, cloning and generation of the MP complementation lines. W.G. and H.S.R. performed expression analysis of the reporter lines. Mi.S. performed the *Arabidopsis* ovule culture and treatments. W.G., H.S.R., B.C. and R.S. generated mutant lines. W.G. and H.S.R. performed the genetic analysis and analysed the data. Me.S., K.B., R.S., D.W. and M.B. provided unpublished material and methods. W.G. and H.S.R. prepared the manuscript. Mi.S. M.B., D.W., Me.S., K.B. and J.F. edited the manuscript prior to submission.

Funding
W.G. is a post-doctoral fellow of the Research Foundation Flanders. H.S.R. is supported by Employment of Best Young Scientists for International Cooperation Empowerment [CZ.1.07/2.3.00/30.0037], co-financed by the European Social Fund and the state budget of the Czech Republic. Mi.S. was funded by the Ramón y Cajal program. This work was supported by the European Research Council [project ERC-2011-StG-20101109-PSDP], project 'CEITEC – Central European Institute of Technology' [CZ.1.05/1.1.00/02.0068], the European Social Fund [CZ.1.07/2.3.00/20.0043] and the Czech Science Foundation GACR [GA13-40637S] to J.F. We acknowledge funding from the Biological and Biotechnological Science Research Council (BBSRC) and Engineering Physics Science Research Council (EPSRC) to R.S. and M.B.

Supplementary material
Supplementary material available online at
http://dev.biologists.org/lookup/suppl/doi:10.1242/dev.115832/-/DC1

References

Bainbridge, K., Guyomarc'h, S., Bayer, E., Swarup, R., Bennett, M., Mandel, T. and Kuhlemeier, C. (2008). Auxin influx carriers stabilize phyllotactic patterning. *Genes Dev.* **22**, 810-823.
Band, L. R., Wells, D. M., Fozard, J. A., Ghetiu, T., French, A. P., Pound, M. P., Wilson, M. H., Yu, L., Li, W., Hijazi, H. I. et al. (2014). Systems analysis of auxin transport in the Arabidopsis root apex. *Plant Cell* **26**, 862-875.
Belmonte, M. F., Kirkbride, R. C., Stone, S. L., Pelletier, J. M., Bui, A. Q., Yeung, E. C., Hashimoto, M., Fei, J., Harada, C. M., Munoz, M. D. et al. (2013). Comprehensive developmental profiles of gene activity in regions and subregions of the Arabidopsis seed. *Proc. Natl. Acad. Sci. USA* **110**, E435-E444.
Bennett, M. J., Marchant, A., Green, H. G., May, S. T., Ward, S. P., Millner, P. A., Walker, A. R., Schulz, B. and Feldmann, K. A. (1996). Arabidopsis AUX1 gene: a permease-like regulator of root gravitropism. *Science* **273**, 948-950.
Berleth, T. and Jürgens, G. (1993). The role of the monopteros gene in organising the basal body region of the Arabidopsis embryo. *Development* **118**, 575-587.
Cole, M., Chandler, J., Weijers, D., Jacobs, B., Comelli, P. and Werr, W. (2009). DORNROSCHEN is a direct target of the auxin response factor MONOPTEROS in the Arabidopsis embryo. *Development* **136**, 1643-1651.
Delbarre, A., Muller, P., Imhoff, V. and Guern, J. (1996). Comparison of mechanisms controlling uptake and accumulation of 2,4-dichlorophenoxy acetic acid, naphthalene-1-acetic acid, and indole-3-acetic acid in suspension-cultured tobacco cells. *Planta* **198**, 532-541.
Friml, J., Benková, E., Blilou, I., Wiśniewska, J., Hamann, T., Ljung, K., Woody, S., Sandberg, G., Scheres, B., Jürgens, G. et al. (2002). AtPIN4 mediates sink-driven auxin gradients and root patterning in Arabidopsis. *Cell* **108**, 661-673.
Friml, J., Vieten, A., Sauer, M., Weijers, D., Schwarz, H., Hamann, T., Offringa, R. and Jürgens, G. (2003). Efflux-dependent auxin gradients establish the apical-basal axis of Arabidopsis. *Nature* **426**, 147-153.
Friml, J., Yang, X., Michniewicz, M., Weijers, D., Quint, A., Tietz, O., Benjamins, R., Ouwerkerk, P. B. F., Ljung, K., Sandberg, G. et al. (2004). A PINOID-dependent binary switch in apical-basal PIN polar targeting directs auxin efflux. *Science* **306**, 862-865.
Furutani, M., Vernoux, T., Traas, J., Kato, T., Tasaka, M. and Aida, M. (2004). PIN-FORMED1 and PINOID regulate boundary formation and cotyledon development in Arabidopsis embryogenesis. *Development* **131**, 5021-5030.
Geldner, N., Friml, J., Stierhof, Y.-D., Jürgens, G. and Palme, K. (2001). Auxin transport inhibitors block PIN1 cycling and vesicle trafficking. *Nature* **413**, 425-428.
Hamann, T., Mayer, U. and Jürgens, G. (1999). The auxin-insensitive bodenlos mutation affects primary root formation and apical-basal patterning in the Arabidopsis embryo. *Development* **126**, 1387-1395.
Hayashi, K.-i., Tan, X., Zheng, N., Hatate, T., Kimura, Y., Kepinski, S. and Nozaki, H. (2008). Small-molecule agonists and antagonists of F-box protein-substrate interactions in auxin perception and signaling. *Proc. Natl. Acad. Sci. USA* **105**, 5632-5637.
Hejátko, J., Blilou, I., Brewer, P. B., Friml, J., Scheres, B. and Benková, E. (2006). In situ hybridization technique for mRNA detection in whole mount Arabidopsis samples. *Nat. Protocols* **1**, 1939-1946.
Hellemans, J., Mortier, G., De Paepe, A., Speleman, F. and Vandesompele, J. (2007). qBase relative quantification framework and software for management and automated analysis of real-time quantitative PCR data. *Genome Biol.* **8**, R19.
Jones, A. R., Kramer, E. M., Knox, K., Swarup, R., Bennett, M. J., Lazarus, C. M., Leyser, H. M. O. and Grierson, C. S. (2008). Auxin transport through non-hair cells sustains root-hair development. *Nat. Cell Biol.* **11**, 78-84.
Joosen, R., Cordewener, J., Supena, E. D. J., Vorst, O., Lammers, M., Maliepaard, C., Zeilmaker, T., Miki, B., America, T., Custers, J. et al. (2007). Combined transcriptome and proteome analysis identifies pathways and markers associated with the establishment of rapeseed microspore-derived embryo development. *Plant Physiol.* **144**, 155-172.
Karimi, M., Bleys, A., Vanderhaeghen, R. and Hilson, P. (2007a). Building blocks for plant gene assembly. *Plant Physiol.* **145**, 1183-1191.
Karimi, M., Depicker, A. and Hilson, P. (2007b). Recombinational cloning with plant gateway vectors. *Plant Physiol.* **145**, 1144-1154.
Kierzkowski, D., Lenhard, M., Smith, R. and Kuhlemeier, C. (2013). Interaction between meristem tissue layers controls phyllotaxis. *Dev. Cell* **26**, 616-628.
Lanková, M., Smith, R. S., Pesek, B., Kubes, M., Zazímalová, E., Petrásek, J. and Hoyerová, K. (2010). Auxin influx inhibitors 1-NOA, 2-NOA, and CHPAA interfere with membrane dynamics in tobacco cells. *J. Exp. Bot.* **61**, 3589-3598.
Le, B. H., Cheng, C., Bui, A. Q., Wagmaister, J. A., Henry, K. F., Pelletier, J., Kwong, L., Belmonte, M., Kirkbride, R., Horvath, S. et al. (2010). Global analysis of gene activity during Arabidopsis seed development and identification of seed-specific transcription factors. *Proc. Natl. Acad. Sci. USA* **107**, 8063-8070.
Ljung, K., Hull, A. K., Celenza, J. L., Yamada, M., Estelle, M., Normanly, J. and Sandberg, G. (2005). Sites and regulation of auxin biosynthesis in Arabidopsis roots. *Plant Cell* **17**, 1090-1104.
Marchant, A., Kargul, J., May, S. T., Muller, P., Delbarre, A., Perrot-Rechenmann, C. and Bennett, M. J. (1999). AUX1 regulates root gravitropism in Arabidopsis by facilitating auxin uptake within root apical tissues. *EMBO J.* **18**, 2066-2073.
Marhavý, P., Bielach, A., Abas, L., Abuzeineh, A., Duclercq, J., Tanaka, H., Pařezová, M., Petrásek, J., Friml, J., Kleine-Vehn, J. et al. (2011). Cytokinin modulates endocytic trafficking of PIN1 auxin efflux carrier to control plant organogenesis. *Dev. Cell* **21**, 796-804.
Marhavý, P., Duclercq, J., Weller, B., Feraru, E., Bielach, A., Offringa, R., Friml, J., Schwechheimer, C., Murphy, A. and Benková, E. (2014). Cytokinin controls polarity of PIN1-dependent auxin transport during lateral root organogenesis. *Curr. Biol.* **24**, 1031-1037.
Parry, G., Delbarre, A., Marchant, A., Swarup, R., Napier, R., Perrot-Rechenmann, C. and Bennett, M. J. (2001). Novel auxin transport inhibitors phenocopy the auxin influx carrier mutation aux1. *Plant J.* **25**, 399-406.
Péret, B., Swarup, K., Ferguson, A., Seth, M., Yang, Y., Dhondt, S., James, N., Casimiro, I., Perry, P., Syed, A. et al. (2012). AUX/LAX genes encode a family of auxin influx transporters that perform distinct functions during arabidopsis Development. *Plant Cell* **24**, 2874-2885.
Petersson, S. V., Johansson, A. I., Kowalczyk, M., Makoveychuk, A., Wang, J. Y., Moritz, T., Grebe, M., Benfey, P. N., Sandberg, G. and Ljung, K. (2009). An auxin gradient and maximum in the Arabidopsis root apex shown by high-resolution cell-specific analysis of IAA distribution and synthesis. *Plant Cell* **21**, 1659-1668.
Petrásek, J. and Friml, J. (2009). Auxin transport routes in plant development. *Development* **136**, 2675-2688.
Rademacher, E. H., Lokerse, A. S., Schlereth, A., Llavata Peris, C. I., Bayer, M., Kientz, M., Freire Rios, A., Borst, J. W., Lukowitz, W., Jürgens, G. et al. (2012). Different auxin response machineries control distinct cell fates in the early plant embryo. *Dev. Cell* **22**, 211-222.
Robert, H. S., Grones, P., Stepanova, A. N., Robles, L. M., Lokerse, A. S., Alonso, J. M., Weijers, D. and Friml, J. (2013). Local auxin sources orient the apical-basal axis in Arabidopsis embryos. *Curr. Biol.* **23**, 2506-2512.
Růzicka, K., Simásková, M., Duclercq, J., Petrásek, J., Zazímalová, E., Simon, S., Friml, J., Van Montagu, M. C. E. and Benková, E. (2009). Cytokinin regulates root meristem activity via modulation of the polar auxin transport. *Proc. Natl. Acad. Sci. USA* **106**, 4284-4289.
Sauer, M. and Friml, J. (2008). In vitro culture of Arabidopsis embryos. *Methods Mol. Biol.* **427**, 71-76.
Sauer, M., Balla, J., Luschnig, C., Wisniewska, J., Reinöhl, V., Friml, J. and Benková, E. (2006a). Canalization of auxin flow by Aux/IAA-ARF-dependent feedback regulation of PIN polarity. *Genes Dev.* **20**, 2902-2911.
Sauer, M., Paciorek, T., Benková, E. and Friml, J. (2006b). Immunocytochemical techniques for whole-mount in situ protein localization in plants. *Nat. Protocols* **1**, 98-103.

Development (2015) 142, 702-711 doi:10.1242/dev.115832

Schlereth, A., Möller, B., Liu, W., Kientz, M., Flipse, J., Rademacher, E. H., Schmid, M., Jürgens, G. and Weijers, D. (2010). MONOPTEROS controls embryonic root initiation by regulating a mobile transcription factor. *Nature* **464**, 913-916.

Spitzer, C., Reyes, F. C., Buono, R., Sliwinski, M. K., Haas, T. J. and Otegui, M. S. (2009). The ESCRT-related CHMP1A and B proteins mediate multivesicular body sorting of auxin carriers in Arabidopsis and are required for plant development. *Plant Cell* **21**, 749-766.

Supena, E. D. J., Winarto, B., Riksen, T., Dubas, E., van Lammeren, A., Offringa, R., Boutilier, K. and Custers, J. (2008). Regeneration of zygotic-like microspore-derived embryos suggests an important role for the suspensor in early embryo patterning. *J. Exp. Bot.* **59**, 803-814.

Swarup, R., Friml, J., Marchant, A., Ljung, K., Sandberg, G., Palme, K. and Bennett, M. (2001). Localization of the auxin permease AUX1 suggests two functionally distinct hormone transport pathways operate in the Arabidopsis root apex. *Genes Dev.* **15**, 2648-2653.

Swarup, R., Kargul, J. J., Marchant, A. A., Zadik, D. D., Rahman, A. A., Mills, R. R., Yemm, A. A., May, S. S., Williams, L. L., Millner, P. P. et al. (2004). Structure-function analysis of the presumptive Arabidopsis auxin permease AUX1. *Plant Cell* **16**, 3069-3083.

Swarup, K., Benková, E., Swarup, R., Casimiro, I., Péret, B., Yang, Y., Parry, G., Nielsen, E., De Smet, I., Vanneste, S. et al. (2008). The auxin influx carrier LAX3 promotes lateral root emergence. *Nat. Cell Biol.* **10**, 946-954.

Ugartechea-Chirino, Y., Swarup, R., Swarup, K., Péret, B., Whitworth, M., Bennett, M. J. and Bougourd, S. (2009). The AUX1 LAX family of auxin influx carriers is required for the establishment of embryonic root cell organization in Arabidopsis thaliana. *Ann. Bot.* **105**, 277-289.

Ulmasov, T., Murfett, J., Hagen, G. and Guilfoyle, T. J. (1997). Aux/IAA proteins repress expression of reporter genes containing natural and highly active synthetic auxin response elements. *Plant Cell* **9**, 1963-1971.

Vieten, A., Vanneste, S., Wiśniewska, J., Benková, E., Benjamins, R., Beeckman, T., Luschnig, C. and Friml, J. (2005). Functional redundancy of PIN proteins is accompanied by auxin-dependent cross-regulation of PIN expression. *Development* **132**, 4521-4531.

Wabnik, K., Robert, H. S., Smith, R. S. and Friml, J. (2013). Modeling framework for the establishment of the apical-basal embryonic axis in plants. *Curr. Biol.* **23**, 2513-2518.

Weijers, D., Schlereth, A., Ehrismann, J. S., Schwank, G., Kientz, M. and Jürgens, G. (2006). Auxin triggers transient local signaling for cell specification in Arabidopsis embryogenesis. *Dev. Cell* **10**, 265-270.

Yoshida, S., de Reuille, P. B., Lane, B., Bassel, G. W., Prusinkiewicz, P. P., Smith, R. S. and Weijers, D. (2014). Genetic control of plant development by overriding a geometric division rule. *Dev. Cell* **29**, 75-87.

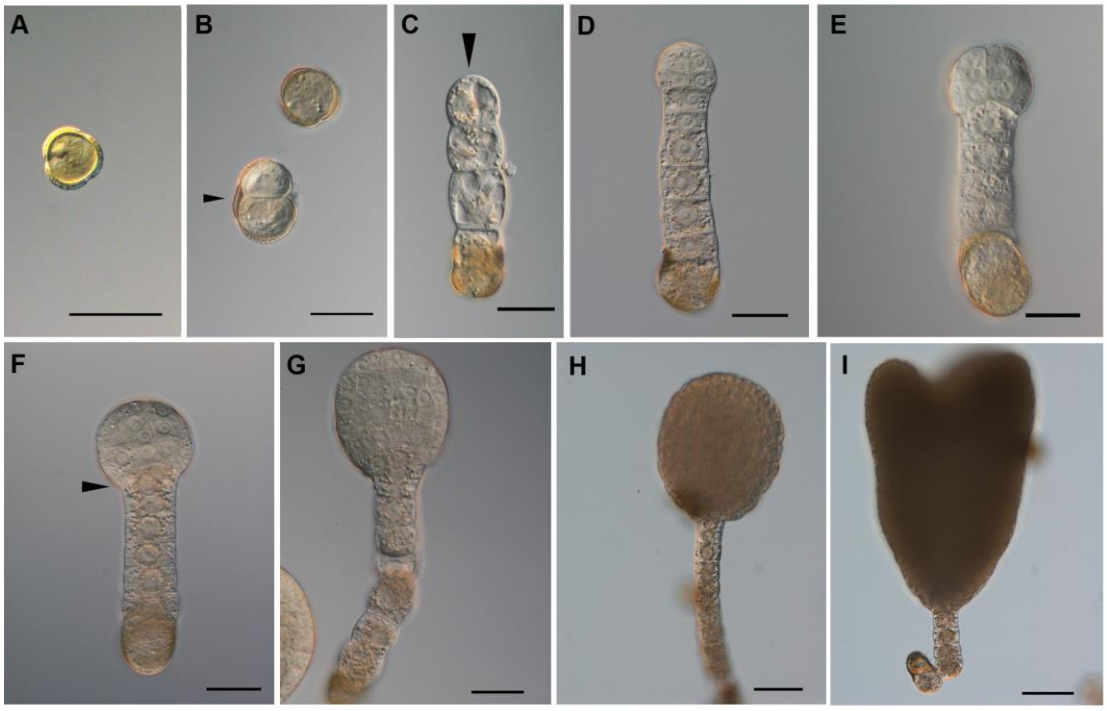

Supplementary material Figure S1. Zygotic development of *Brassica napus* microspore-induced embryos

Brassica napus microspore-induced embryogenesis follows a zygotic embryo development from pollen grain (A). After heat shock, the pollen grain divides (B) and germinates a suspensor-like structure. The apical cell divides vertically (C, arrowhead) and follows a zygotic embryogenesis development: 8-cell (D), 16-cell (E), globular (F, the arrowhead shows the hypophysis), late globular (G, H) and heart stages (I). Scale bars represent 30 µm in A-G and 60 µm in H-I.

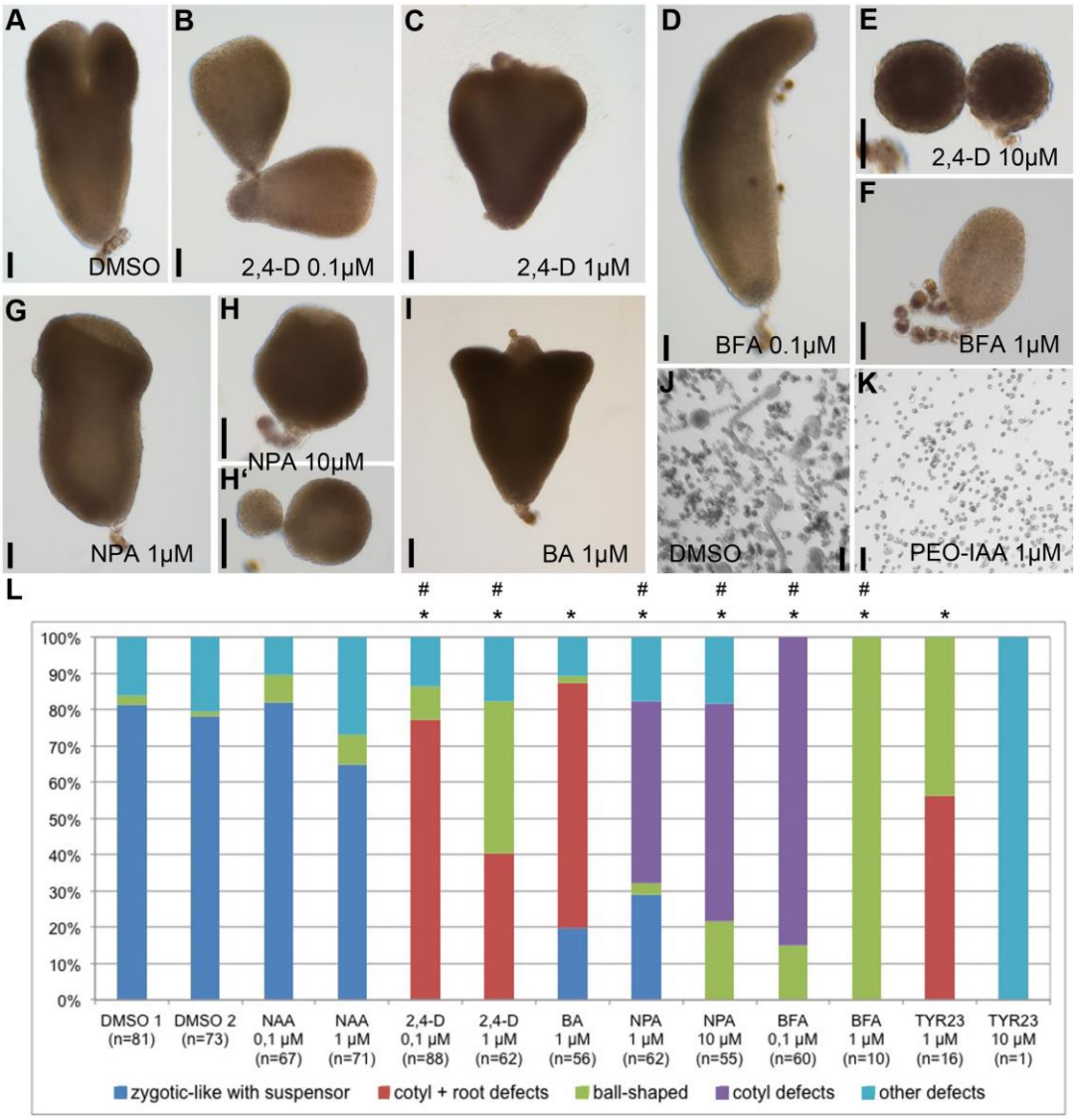

Supplementary material Figure S2. Treatments of *Brassica napus* microspore-induced embryos

Brassica napus microspore-induced embryos were treated 5 days after heat shock with DMSO (A) for control, with 2,4-D at 0.1 µM (B), 1 µM (C) and 10 µM (E), brefeldin A (BFA) at 0.1 µM (D) and 1 µM (F), with NPA at 1 µM (G) and 10 µM (H, H'), and with the cytokinin BA at 1 µM (I). Microspore did not germinate when treated with PEO-IAA at 1 µM (K, DMSO for control in J). In L, a graph summarizes the observed phenotypes for the presented treatments (A-I), in addition to NAA at 0.1 µM and 1 µM and to tyrphostin A23 (TyrA23) at 1 µM and 10 µM. Scale bars represent 50 µm. Significant difference ($P < 0.03$) between DMSO controls and the treatment (*) or between the two concentrations of one compound (#) is indicated above the graph (L).

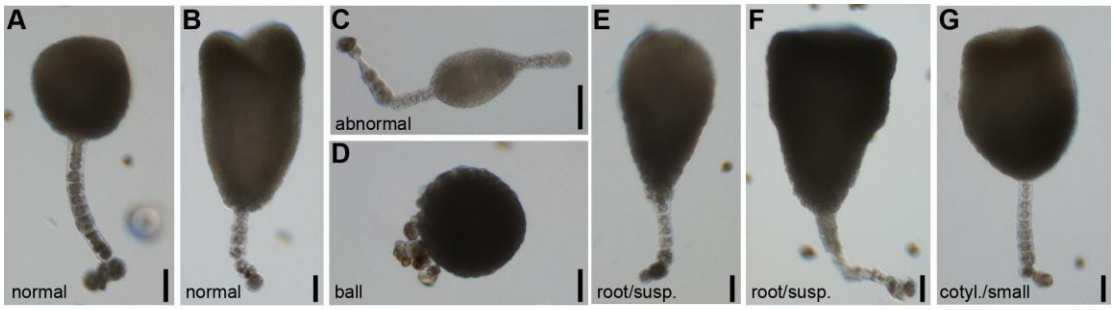

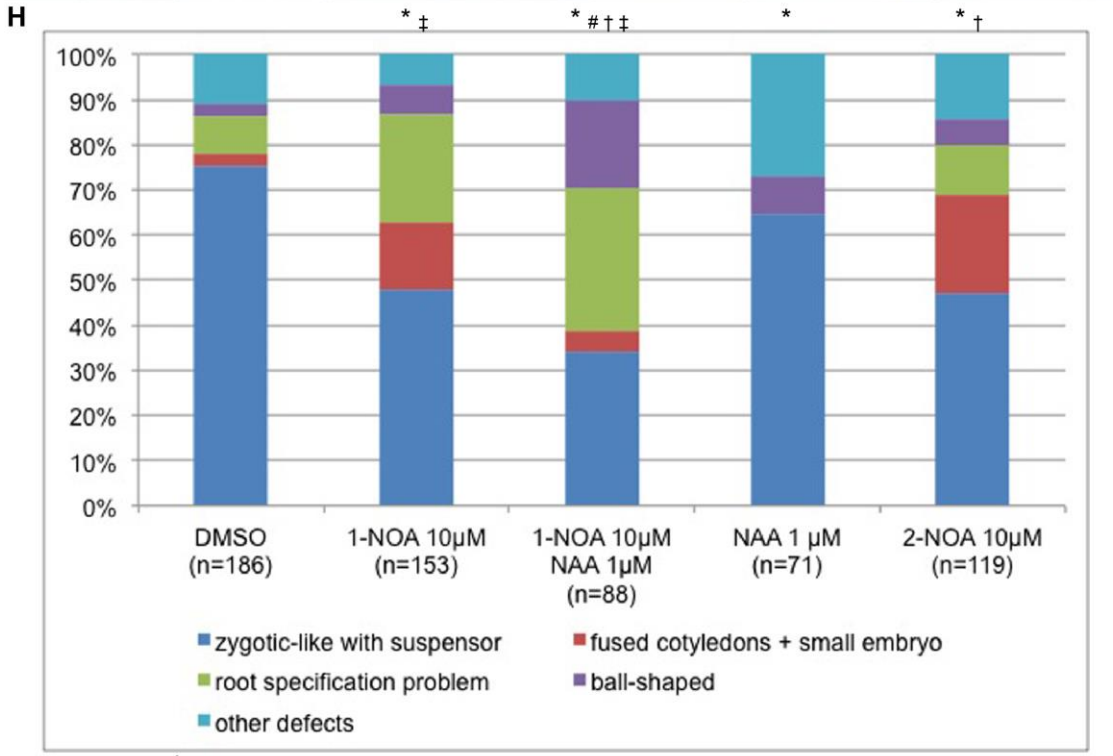

I

	zygotic-like	fused cotyl./small	root defects	ball-shaped	other defects
DMSO	75.3	2.7	8.6	2.7	10.8
1-NOA	47.7	15.0	24.2	6.5	6.5
1-NOA + NAA	34.1	4.5	31.8	19.3	10.2
NAA	64.8	0.0	0.0	8.5	26.8
2-NOA	47.1	21.8	10.9	5.9	14.3

Supplementary material Figure S3. Blocking auxin influx in *Brassica napus* microspore-induced embryos

Five days after heat-shock induction several compounds were added to *Brassica napus* microspore-induced embryos: 1-NOA at 10 µM, NAA at 1 µM, 1-NOA at 10 µM and NAA at 1 µM together or 2-NOA at 10 µM with DMSO as control. Embryonic phenotypes were scored in the following categories: zygotic-like embryos with suspensor (e.g. normal, A, B, dark blue in H), abnormal embryos or with other defects (C, light blue in H), ball-shaped embryos (D, purple in H), embryos with root

or suspensor specification problem (E, F, green in H), embryos with fused cotyledons or smaller size (G, red in H). The quantification is summarized in graph (H) and table (I). Scale bars represent 50 µm. Significant difference ($P < 0.03$) compared DMSO controls (*), to 1-NOA (†), to 2-NOA (‡) and to NAA (#) is indicated above the graph (H).

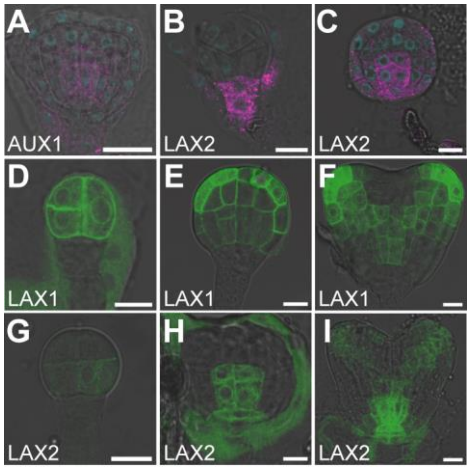

Supplementary material Figure S4. Expression patterns of *AUX1*, *LAX1* and *LAX2*

Immuno-localization using anti-HA in *pAUX1::AUX1-HA* embryos (A) and anti-LAX2 in WT embryos (B, C) indicated that *AUX1* is expressed in provascular cells (A) and that *LAX2* in suspensor at early globular stage (B) and in provascular cells from late globular onward (C). The signal is displayed in magenta, nuclei, in cyan, are counter-stained by DAPI. Expression patterns of *LAX1* and *LAX2* are shown after confocal imaging of embryos of *pLAX1::LAX1-Venus* (D-F) and of *pLAX2::LAX2-Venus* (G-I) plants. Signal is at the plasma membrane with noticeable intracellular signal, putatively at the endoplasmic reticulum. Also antibodies against LAX2 give a strong background noise signal. Scale bars represent 10 µm.

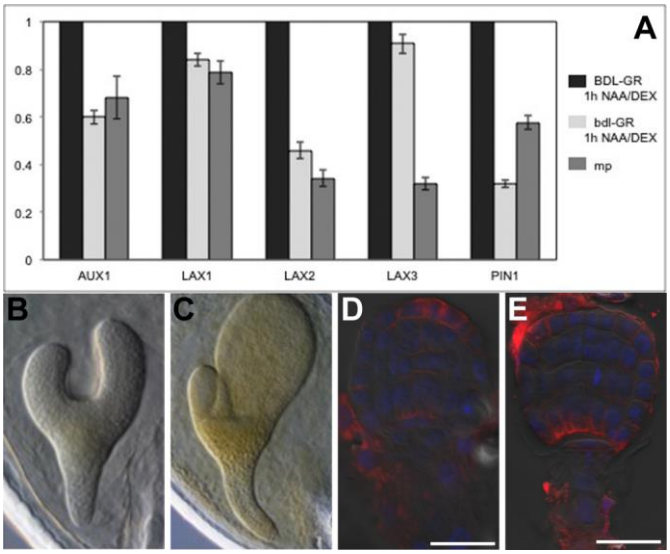

Supplementary material Figure S5. MP/BDL transcriptional pathway regulates *AUX1, LAX2* and *PIN1* expression

(A) Graph reporting qRT-PCR results testing *AUX1*, *LAX1*, *LAX2*, *LAX3* and *PIN1* expressions in *pRPS5A::BDL-GR* and *pRPS5A::bdl-GR* roots, after 1 h of co-incubation of dexamethasone (DEX) and NAA, and mp^{B4149} seedlings. (B) mp^{B4149} embryo. (C) *aux1 lax1 lax2* embryo. (D, E) PIN1 immunolocalization of PIN1 (red signal) in wild type (D) and in *pMP::PIN1 PWiii30* (E) embryos. The intensity of PIN1 signal is higher in *pMP::PIN1* embryos (9/15) compared to wild type. Nuclei are stained by DAPI in blue. Scale bars represent 20 µm.

Supplementary material Table S1. Quantification of all mutant embryonic phenotypes.

Experiment/Ghent Line	n	normal (%)	defects (%)				
			cotyl.	root	cotyl+root	mp-like	total
pin1-201/+	189	81.5	18.0	0.5	0	0	18.5
pin4-2	186	88.2	0	0	11.8	0	11.8
aux1 lax1 lax2	443	73.8	9.5	4.3	9.9	2.5	26.2
pin1-201/+ aux1 lax1 lax2	213	55.9	21.6	8.9	10.8	2.8	44.1
pin4-2 aux1 lax1 lax2	123	60.2	0	0	39.8	0	39.8
Experiment/Brno							
Col	188	100	0	0	0	0	0
pin1-201/+	353	87.5	12.5	0	0	0	12.5
pin4-2	140	97.9	2.1	0	0	0	2.1
pin4-3	195	97.4	2.6	0	0	0	2.6
aux1 lax1 lax2	459	92	1.1	7	0	0	8.1
pin1-201/+ aux1 lax1 lax2	129	86.1	12.4	1.6	0	0	14
pin4-2 aux1 lax1 lax2	304	95.1	1	3.9	0	0	4.9
pin4-3 aux1 lax1 lax2	136	88.2	3.7	8.1	0	0	11.8
pin1-201/+ pin4-2 aux1 lax1 lax2	1424	73.6	25.8	0.6	0	0	26.4
PIN1 pin4-2 aux1 lax1 lax2 (from *pin1/+ pin4 aux1 lax1 lax2*)	432	94.9	4.1	1	0	0	5.1

Embryos were scored from globular to heart stages in two to three biological repeats per growth locations.

Statistic table related to data in Table S1

Fisher Exact test	Chi-square	df	P	Significant difference
aux1 lax1 lax2 Ghent vs Brno	99.2	4	0	yes
Col vs *aux1 lax1 lax2* Brno	16.1	2	0	yes
Col vs *pin1* Brno	25.5	1	0	yes
Col vs *pin4-2* Brno	4.07	1	0.044	yes
Col vs *pin4-3* Brno	4.88	1	0.027	yes
pin4-2 vs *pin4-3* Brno	0.062	1	0.803	no
pin1 vs *pin1 aux1 lax1 lax2* Ghent	50.2	4	0	yes
pin1 vs *pin1 aux1 lax1 lax2* Brno	5.5	2	0,064	no
aux1 lax1 lax2 vs *pin1 aux1 lax1 lax2* Ghent	28	4	0	yes
aux1 lax1 lax2 vs *pin1 aux1 lax1 lax2* Brno	4.6	2	0	yes
pin4-2 vs *pin4-2 aux1 lax1 lax2* Ghent	32,8	1	0	yes
pin4-2 vs *pin4-2 aux1 lax1 lax2* Brno	6.55	2	0,038	yes
pin4-3 vs *pin4-3 aux1 lax1 lax2* Brno	16.8	2	0	yes
aux1 lax1 lax2 vs *pin4-2 aux1 lax1 lax2* Ghent	74.9	4	0	yes
aux1 lax1 lax2 vs *pin4-2 aux1 lax1 lax2* Brno	3.11	2	0.211	no
aux1 lax1 lax2 vs *pin4-3 aux1 lax1 lax2* Brno	4.52	2	0.104	no
pin4-2 aux1 lax1 lax2 vs *pin4-3 aux1 lax1 lax2* Brno	7.29	2	0.026	yes
pin4-2 aux1 lax1 lax2 Ghent vs Brno	83.7	1	0	yes
aux1 lax1 lax2 vs *pin1 pin4 aux1 lax1 lax2* Brno	186	2	0	yes
pin1 vs *pin1 pin4 aux1 lax1 lax2* Brno	31.1	2	0	yes

pin1 aux1 lax1 lax2 vs *pin1 pin4 aux1 lax1 lax2* Brno	12.4	2	0.002	yes
pin4 aux1 lax1 lax2 vs *pin1 pin4 aux1 lax1 lax2* Brno	109	2	0	yes
PIN1 pin4 aux1 lax1 lax2 vs *pin1 pin4 aux1 lax1 lax2* Brno	94.2	2	0	yes
pin4 aux1 lax1 lax2 vs *PIN1 pin4 aux1 lax1 lax2* Brno	13.8	2	0.001	yes

Supplementary material Table S2. Quantification of seedling phenotypes in all mutants

Experiment/Ghent			cotyl. defects with normal root (%)					*mp*-like
Line	n	normal	tricot	monocot	no cotyl/stub	other	total	(%)
pin1-201/+	302	91.7	3.3	1	0	4	8.3	0
pin4-2	382	98.5	0.5	0	0	1	1.5	0
aux1 lax2	360	100	0	0	0	0	0	0
aux1 lax1 lax2	406	88.2	1.2	4.2	0.5	2.2	8.1	3.7
pin1-201/+ aux1 lax1 lax2	322	69.2	1.2	8.4	18.4	1.6	29.6	1.2
pin4-2 aux1 lax2	210	95.6	0	1.9	0.5	1	3.4	1
pin4-2 aux1 lax1 lax2	366	93	0.5	3.6	0	1.6	5.7	1.3
Experiment/Brno								
Col	440	100	0	0	0	0	0	0
pin1-201/+	458	94.8	3.7	1.3	0	0.2	5.2	0
pin4-2	173	99.4	0	0.6	0	0	0.6	0
pin4-3	437	100	0	0	0	0	0	0
aux1 lax1 lax2	289	91.7	0.3	2.8	0	0.3	3.5	4.8
pin1-201/+ aux1 lax1 lax2	554	71.5	0	7.6	19.9	0.5	28	0.5
pin4-2 aux1 lax1 lax2	349	95.1	0	2.9	1.1	0.3	4.3	0.6
pin1-201/+ pin4-2 aux1 lax1 lax2	1978	81.4	0.1	4.9	12.6	0.9	18.5	0.1
PIN1 pin4-2 aux1 lax1 lax2 (from *pin1/+ pin4 aux1 lax1 lax2*)	424	94.7	0.2	3.3	0.7	0.9	5.1	0.2

Statistic table related to data in Table S2

Fisher Exact test 3x2	Chi-square	df	P	Significant difference
aux1 lax1 lax2 Brno vs Ghent	6.7	2	0.035	yes
pin1 vs *pin1 aux1 lax1 lax2* Ghent	50.1	2	0	yes
pin1 vs *pin1 aux1 lax1 lax2* Brno	92.3	2	0	yes
aux1 lax1 lax2 vs *pin1 aux1 lax1 lax2* Ghent	58.9	2	0	yes
aux1 lax1 lax2 vs *pin1 aux1 lax1 lax2* Brno	85.7	2	0	yes
pin4-2 vs *pin4-2 aux1 lax1 lax2* Ghent	14.8	2	0.001	yes
pin4-2 vs *pin4-2 aux1 lax1 lax2* Brno	6.43	2	0.04	yes
aux1 lax1 lax2 vs *pin4-2 aux1 lax1 lax2* Ghent	6.07	2	0.048	yes
aux1 lax1 lax2 vs *pin4-2 aux1 lax1 lax2* Brno	12	2	0.003	yes
aux1 lax1 lax2 vs *pin1 pin4 aux1 lax1 lax2* Brno	118	2	0	yes
PIN1 pin4 aux1 lax1 lax2 vs *pin1 pin4 aux1 lax1 lax2* Brno	45.6	2	0	yes

Supplementary material Table S3. Quantification of *mp^{S319}* phenotypes in *aux/lax* background

Embryonic defects/Ghent			P from contingency table X^2 tests compared to		
Line	n	% defects	Col	*mp^{S319}*/+	*aux/lax*
Col	340	0.0			
aux1-21	87	2.3	0.005		
aux1 lax2	260	1.5	0.022		
aux1 lax1 lax2	56	21.4	0.000		
mp^{S319}/+	281	6.1	0.000		
mp/+ aux1	393	7.4	0.000	0.5	0.081
mp/+ aux1 lax2	450	13.6	0.000	0.001	0.000
mp/+ aux1 lax1 lax2	216	27.3	0.000	0.000	0.371
Seedlings defects/Ghent	n	% rootless seedlings	% total defective seedlings	Col	*mp^{S319}*/+	*aux/lax*
Col	285	0.0	0.0			
aux1	465	0.0	0.0	/		
aux1 lax1	643	0.6	2.3	0.009		
aux1 lax2	635	0.0	0.0	/		
aux1 lax1 lax2	502	3.6	8.7	0.000		
mp^{S319}/+	821	4.6	5.2	0.000		
mp/+ aux1	1018	6.1	7.5	0.000	0.000	0.03
mp/+ aux1 lax1	465	10.5	17.4	0.000	0.000	0.000
mp/+ aux1 lax2	678	9.0	10.4	0.000	0.000	0.000
mp/+ aux1 lax1 lax2	504	14.2	22.0	0.000	0.000	0.000

Embryos were scored from globular to heart stages. All deviations to the wild-type embryo development are collected.

Seedling defects include aberrant number and symmetry of cotyledons (monocot., tricot., no cotyledons, one smaller cotyledon) and rootless seedlings similar to *mp* typical phenotype (see Fig. 5G) with three, two, one or no cotyledons.

Contingency table X^2 statistical tests were performed for statistical analysis. Mutants were tested against Col. Lines resulting of the crosses with *mp/+* were tested against Col and against corresponding *aux/lax* mutant combinations. Significant difference is observed for $P < 0.05$.

Supplementary material Table S4. Analysis of lines with *MP*-driven expression of *PIN1*, *AUX1* and *LAX2* in *mp* alleles

Line in T2	% rootless in T2/Ghent (n)	% rootless in T3 homoz./Brno (n)	qPCR results
ASi29	18.3 (120)		1.99 ± 0.14
ASi36	18.4 (87)	21.7 (507)	
ASi17	20.8 (125)		
ASi25	21.6 (134)		
ASi26	21.9 (137)		
ASi2	23.4 (124)		
ASiii1	23.5 (81)		
ASiii2	23.8 (84)		
ASi17	24.1 (108)		
ASi6	24.5 (106)		
ASi4	25.0 (116)		
ASiii5	25.5 (145)		
ASi32	26.3 (156)		
ASi42	26.4 (106)		
ASi3	26.5 (121)		
ASi14	26.5 (102)		
ASi30	26.6 (143)		1.47 ± 0.13
ASiii9	27.4 (135)		
ASiii7	27.9 (154)	22.5 (608)	2.01 ± 0.19
ASi9	28 (168)		
ASiii6	28.2 (156)	25.2 (1440)	3.91 ± 0.40
ASi23	28.2 (131)		
ASi24	29 (138)		
ASi11	29.5 (210)		
ASiii4	31.4 (153)		
ASiii3	32.3 (155)		
ASi39	32.6 (129)		
LSii45	12.7 (63)		
LSii39	18.2 (66)		
LSi51	18.7 (75)		
LSii22	19.8 (91)		
LSii41	20.5 (83)		
LSi48	21.1 (71)		
LSii48	21.1 (71)		
LSii38	22. (77)		
LSi50	22.9 (70)		
LSii7	23.3 (103)		
LSii44	24.4 (78)		
LSii40	24.7 (73)		
LSii26	24.7 (81)		
LSii16	25 (80)		
LSii21	25.7 (113)		
LSii34	25.7 (66)		
LSii14	26.2 (84)		

LSii32	26.8 (71)	29 (965)	9.32 ± 0.60
LSii3	27.3 (77)		
LSii15	27.4 (102)	23 (643)	11.20 ± 0.73
LSii42	27.5 (80)		
LSii28	27.8 (72)		6.84 ± 0.39
LSii9	28.1 (64)		
LSii5	28.7 (150)		
LSii17	29.1 (86)		
LSi46	29.8 (67)	22 (723)	4.40 ± 0.31
LSii13	30.6 (98)		
LSii25	31.9 (94)		
LSii12	32.6 (86)		
LSii8	33.3 (75)		
LSi49	33.8 (77)		
PSiii26	12.2 (82)		
PSiii17	15.7 (70)	24.5 (1687)	4.13 ± 0.18
PSiii21	20.5 (73)		
PSiii10	21.6 (74)	26.9 (659)	6.29 ± 0.34
PSiii23	21.8 (78)		1.55 ± 0.21
PSiii14	23.3 (60)		
PSiii18	24.1 (83)		
PSiii19	25 (52)		1.35 ± 0.07
PSiii22	25.7 (74)		
PSiii13	25.7 (70)		
PSiii15	26.9 (78)		
PSiii25	29.1 (55)		
PSiii16	29.7 (64)		
AWv10	3.8 (106)		
AWiv1	4.1 (172)	6.2 (64)	3.12 ± 0.29
AWiv15	5.8 (257)		
AWv37	5.9 (101)		
AWv43	6 (100)		
AWv9	6.2 (160)		
AWiv21	7 (157)		
AWv24	7 (156)		
AWv36	7.1 (99)		
AWv35	7.1 (211)		
AWv25	7.6 (171)		
AWv4	7.8 (128)		
AWiv4	7.9 (152)		
AWiv18	8.1 (271)		
AWiv11	8.1 (184)		
AWv49	8.2 (97)		
AWiv20	8.3 (133)		2.25 ± 0.15
AWv38	8.3 (72)		
AWiv13	8.8 (193)		
AWiv11	9.3 (216)		
AWv26	9.7 (144)		

AWv42	10.3 (126)		
AWv34	10.4 (144)		
AWiv19	10.5 (295)		
AWv41	11.0 (154)		
AWv50	11.1 (280)		
AWv45	11.3 (141)	15.4 (635)	2.85 ± 0.18
AWiv6	11.5 (226)		
AWv21	11.9 (118)		
AWv40	13.3 (105)	13.5 (1061)	2.14 ± 0.17
AWv14	13.8 (130)		
AWv12	17.4 (167)	8.3 (779)	
AWiv12	18.9 (185)	5.9 (477)	3.06 ± 0.20
LWv7	1.7 (59)		
LWvi17	3.7 (81)		
LWvi42	4.6 (65)		
LWv8	4.8 (84)		
LWvi4	7.5 (67)		
LWiv31	7.8 (115)		
LWv3	8.6 (81)		
LWvi46	10 (60)		
LWvi44	11.1 (72)	5.2 (306)	3.16 ± 0.23
LWvi6	11.1 (72)		
LWvi21	11.6 (112)		
LWvi24	12 (108)		
LWvi9	12.2 (90)		
LWvi50	13.4 (67)		
LWvi23	14.4 (90)		
LWv4	15.1 (73)		
LWv1	15.4 (78)		7.23 ± 0.51
LWv6	15.8 (57)		
LWvi18	15.8 (82)		
LWvi1	16 (50)	12.9 (923)	
LWv5	16.7 (42)		
LWvi14	16.7 (66)		
LWvi5	17.1 (41)		
LWvi37	17.3 (75)		
LWvi32	19.2 (78)		
LWv2	19.6 (51)	19 (231)	3.29 ± 0.27
LWvi13	21.3 (61)		1.54 ± 0.07
LWvi49	26.9 (67)		
LWvi2	30.8 (65)	24.8 (459)	
PWiii33	4.2 (215)		
PWvii51	5 (139)		
PWvii7	5.1 (158)		
PWiii36	6 (218)		
PWiii32	6.5 (138)		
PWvii21	6.5 (138)		
PWvii12	6.6 (121)		

PWvii41	6.9 (116)		
PWvii24	7.5 (147)		
PWvii14	7.8 (166)		
PWiii37	8 (175)		
PWvii1	8.3 (109)		1.40 ± 0.11
PWvii2	8.3 (133)		1.68 ± 0.1
PWvii13	9.4 (138)		
PWvii30	9.5 (116)		14.99 ± 0.68
PWvii32	10 (110)		
PWvii19	10.2 (137)		
PWvii18	10.3 (146)		
PWiii35	11.3 (194)		
PWiii30	11.5 (148)	8.7 (681)	
PWvii36	11.5 (139)		
PWiii29	11.6 (147)		
PWvii15	13.7 (122)		
PWvii39	13.7 (139)	10.5 (153)	
PWvii31	14.4 (118)		
PWiii41	16.3 (147)		
PWvii23	19 (105)		3.60 ± 0.20
PWvii22	19.3 (93)		

A = MP::AUX1
L = MP::LAX2
P = MP::PIN1
S = mp^{B4149}/+ background
W = mp^{S319}/+ background
i-vii = tray number of the T1
1-51 = plant number of the T1

Supplementary material Table S5. Results of crosses between *MP::PIN1* and *MP::AUX1* or *MP::LAX2* in mp^{B4149} strong allele. Analysis done in Brno.

Lines					cot. defects with normal root (%)			*mp*-like seedlings (%)			
maternal	x	paternal	n	normal	monocot.	other defects/stub	total	dicot.	monocot.	fused cot.	total
AS	x	*PS*	538	71.6	0	3.9	**3.9**	12.1	11.1	1.3	**24.5**
AS	x	*mp*	26	69.2	0	7.7	7.7	19.2	3.9	0	23.1
AS	x	*AS*	2769	72.4	0.1	3.1	3.2	17.2	6.3	0.9	24.4
LS	x	*PS*	166	71.8	0.6	6	**6.6**	10.2	9.6	1.8	**21.6**
LS	x	*mp*	100	71	0	8	8	11	10	0	21
LS	x	*LS*	1230	73.4	0.4	2.4	2.8	17.2	5.7	0.9	23.8
PS	x	*PS*	903	77.1	0	0.2	0.2	15.3	7.4	0	22.7

At least two independent T3 homozygous lines for each *pMP:xx* lines ectopically expressing *AUX1* (*AS*), *LAX2* (*LS*) and *PIN1* (*PS*) in mp^{B4149} strong allele (*S*) background were crossed to each other (*PIN1* to *AUX1*, *AS* x *PS* and *PIN1* to *LAX2*, *LS* x *PS*). Control crosses are selfed *pMP::AUX1* (*AS* x *AS*), *pMP::LAX2* (*LS* x *LS*), *pMP::PIN1* (*PS* x *PS*) and backcrosses to mp^{B4149} (*AS* x *mp*, *LS* x *mp*). Seedling phenotypes were scored 5 days after germination. Contingency table X^2 statistical tests were performed for statistical analysis.

3x2 contingency table	Chi-square	df	P	Significant difference
AS x PS vs *AS x mp*	0.914	2	0.633	no
AS x PS vs *AS x AS*	0.367	2	0.832	no
AS x PS* vs *PS x PS	30.5	2	0	**yes**
LS x PS vs *LS x mp*	0.0537	2	0.974	no
LS x PS* vs *LS x LS	9.37	2	0.009	**yes**
LS x PS* vs *PS x PS	53.3	2	0	**yes**
AS x PS vs *LS x PS*	3.63	2	0.163	no

Supplementary material Table S6. Results of crosses between *MP::PIN1* and *MP::AUX1* or *MP::LAX2* in *mp*^{S319} weak allele. Analysis done in Brno.

Lines					cot. defects with	*mp*-like seedlings (%)			
maternal	x	paternal	n	normal	normal root (%)	dicot.	monocot.	fused cot.	total
AW	x	*PW*	766	83.3	0.4	12.1	3.9	0.3	**16.3**
PW	x	*AW*	764	81.3	0.8	11.6	5.5	0.8	**17.9**
AW	*x*	*mp*	292	94.9	1	3.4	0.7	0	4.1
mp	x	*AW*	367	83.9	1.4	12	1.1	1.6	14.7
AW	x	*AW*	656	84.1	0.3	14.2	1.1	0.3	15.5
LW	x	*PW*	519	79.6	0.6	9.6	9.8	0.4	**19.8**
PW	x	*LW*	861	83.6	0.6	8.1	6.3	1.4	**15.8**
LW	*x*	*mp*	279	83.9	0.7	8.6	5.4	1.4	15.4
mp	x	*LW*	353	90.9	0.3	4.5	3.7	0.6	8.8
LW	x	*LW*	430	85.8	0.2	11.9	2.1	0	14
PW	*x*	*mp*	240	75	0	18.8	5.4	0.8	25
mp	x	*PW*	360	82.7	0.3	10.8	5.6	0.6	17
PW	x	*PW*	731	82.4	1.9	9	5.7	1	15.7
mp	*x*	*mp*	580	89.1	0.2	9	1.7	0	10.7

At least two independent T3 homozygous lines for each *pMP:xx* lines ectopically expressing *AUX1* (*AW*), *LAX2* (*LW*) and *PIN1* (*PW*) in *mp*^{S319} weak allele (*W*) background were crossed to each other (*PIN1* to *AUX1*, *AW* x *PW* and *PIN1* to *LAX2*, *LW* x *PW*). Control crosses are selfed *pMP::AUX1* (*AW* x *AW*), *pMP::LAX2* (*LW* x *LW*), *pMP::PIN1* (*PW* x *PW*), *mp* and backcrosses to *mp*^{S319} (*AW* x *mp*, *mp* x *AW*, *LW* x *mp*, *mp* x *LW*, *PW* x *mp*, *mp* x *PW*). Seedling phenotypes were scored 5 days after germination. Contingency table X^2 statistical tests were performed for statistical analysis.

3x2 contingency table	Chi-square	df	P	Significant difference
AW x PW vs *PW x AW*	1.78	2	0.411	no
AW x mp* vs *mp x AW	20.6	2	0	**yes**
AW x PW* vs *AW x mp	29.1	2	0	**yes**
PW x AW vs *mp x pAW*	2.58	2	0.275	no
AW x PW vs *AW x AW*	0.238	2	0.888	no
PW x AW vs *AW x AW*	2.99	2	0.225	no
AW x mp* vs *AW x AW	26.6	2	0	**yes**
mp x AW vs *AW x AW*	3.96	2	0.138	no
AW x PW* vs *mp x mp	9.38	2	0.009	**yes**
PW x AW* vs *mp x mp	16.5	2	0	**yes**
AW x PW* vs *PW x PW	7.77	2	0.021	**yes**
PW x AW vs PW x PW	4.69	2	0.096	no

LW x PW vs *PW x LW*	3.71	2	0.156	no
LW x mp* vs *mp x LW	7.35	2	0.025	**yes**
LW x PW vs *LW x mp*	2.42	2	0.298	no
PW x LW* vs *mp x LW	11	2	0.004	**yes**
LW x PW* vs *LW x LW	6.53	2	0.038	**yes**
PW x LW vs *LW x LW*	1.55	2	0.46	no
LW x mp vs *LW x LW*	1.26	2	0.532	no
mp x LW vs *LW x LW*	5.06	2	0.08	no
LW x PW* vs *mp x mp	19.5	2	0	**yes**
PW x LW* vs *mp x mp	9.19	2	0.01	**yes**
LW x PW* vs *PW x PW	7.22	2	0.027	**yes**
PW x LW* vs *PW x PW	5.98	2	0.05	**yes**
AW x AW* vs *mp x mp	6.59	2	0.037	**yes**
LW x LW vs *mp x mp*	2.53	2	0.282	no
PW x PW* vs *mp x mp	16.4	2	0	**yes**
AW x AW vs *LW x LW*	0.577	2	0.749	no
AW x AW* vs *PW x PW	7.91	2	0.019	**yes**
LW x LW* vs *PW x PW	6.89	2	0.032	**yes**

Supplementary material Table S7. Primers

Genotyping

Gene/alleles		
lax1	Forward primer	ATATGGTTGCAGGTGGCACA
	Reverse primer	GTAACCGGCAAAAGCTGCA
	Border primer	AAGCACGACGGCTGTAGAATAG
lax2	Forward primer	ATGGAGAACGGTGAGAAAGCAGC
	Reverse primer	CGCAGAAGGCAGCGTTAGCG
	Border primer	AAGCACGACGGCTGTAGAATAG
lax3	Forward primer	TACTTCACCGGAGCCACCA
	Reverse primer	TGATTGGTCCGAAAAAGG
	Border primer	AAGCACGACGGCTGTAGAATAG
pin1-201	Forward primer	CAAAAACACCCCCAAAATTTC
	Reverse primer	AATCATCACAGCCACTGATCC
	Border primer	TGGTTCACGTAGTGGGCCATCG
pin4-2	Forward primer	AACCGGTACGGGTGTTTCAACTA
	Reverse primer	GCCATTCCAAGACCAGCATCT
	Border primer	GAGCGTCGGTCCCCACACTTCTATAC
pin4-3	Forward primer	AACCGGTACGGGTGTTTCAACTA
	Reverse primer	GCCATTCCAAGACCAGCATCT
	Border primer	GAGCGTCGGTCCCCACACTTCTATAC
mp^{B4149}	Forward primer	CTCTCAGCGGATAGTATGCACATCGG
	Reverse primer	ATGGATGGAGCTGACGTTTGAGTTC
	Resctriction	MseI, cut in mp^{B4149}
mp^{S319}	Forward primer	GATTTTCCAGATAATTCTGGA
	Reverse primer	ATGAATATAGTTTCAGGTCTC
	Border primer	ATTTTGCCGATTTCGGAAC

Cloning primers (attB cassettes underlined)

attB4_MP_FOR	GGGGACAACTTTGTATAGAAAAGTTGCCGACGTGTGTGAATTACCAAGGCG

attB1R_MP_REV	GGGGACTGCTTTTTTGTACAAACTTGCCATCATACAGAGAGATTTTTCAATG
attB1_PIN1_FOR	GGGGACAAGTTTGTACAAAAAAGCAGGCTTCATGATTACGGCGGCGGACTTCTACCACG
attB2R_PIN1_REV	GGGGACCACTTTGTACAAGAAAGCTGGGTGTCATAGACCCAAGAGAATGTAGTAGAG
attB1_AUX1_FW	GGGGACAAGTTTGTACAAAAAAGCAGGCTTCATGTCGGAAGGAGTAGAAGCGATAGTAGC
attB2R_AUX1_RV	GGGGACCACTTTGTACAAGAAAGCTGGGTGTCAAAGACGGTGGTGTAAAGCGGAGACC
attB1_LAX2_FW	GGGGACAAGTTTGTACAAAAAAGCAGGCTTCATGGAGAACGGTGAGAAAGCAGC
attB2R_LAX2_RV	GGGGACCACTTTGTACAAGAAAGCTGGGTGTCAAAGGCCGTGAGTGTGATTGAAG

qPCR/RNA *in situ* probe

AUX1-ISH	Forward	CCAAGCTTCTAATACGACTCACTATAGGGAGATGCAGCCGCCGCACATGC
	Reverse	GTTCATGGTAAAATAGTTTATATAAG
AUX1-qPCR	Forward	ATGACAACGGAACAGATCAG
	Reverse	GTGCCATAGGAAATTGCTTAG
LAX1-qPCR	Forward	TACTCCGAGACCTTCCAACTACG
	Reverse	TCCACCGCCACCACTTCC
LAX2-qPCR	Forward	GGAGAACGGTGAGAAAGC
	Reverse	TCAGATAGCTTAGATTTGATGTC
PIN1-qPCR	Forward	TACTCCGAGACCTTCCAACTACG
	Reverse	TCCACCGCCACCACTTCC
EEF1α4	Forward	CTGGAGGTTTTGAGGCTGGTAT
	Reverse	CCAAGGGTGAAAGCAAGAAGA
CDKA	Forward	ATTGCGTATTGCCACTCTCATAGG
	Reverse	TCCTGACAGGGATACCGAATGC